NEW OBSERVATIONS ON FLASH BAINITE

by

Petch Janbanjong

Bachelor of Engineering in Mechanical Engineering, KMITL, Thailand, 2011

Submitted to the Graduate Faculty of

Swanson School of Engineering in partial fulfillment

of the requirements for the degree of

Master of Science

University of Pittsburgh

2016

UNIVERSITY OF PITTSBURGH

SWANSON SCHOOL OF ENGINEERING

This thesis was presented

by

Petch Janbanjong

It was defended on

March 30, 2016

and approved by

Luis E. Vallejo, Ph.D., Professor, Department of Civil and Environmental Engineering

Patrick Smolinski, Ph.D., Associate Professor, Department of Mechanical Engineering and Materials Science

Anthony J. DeArdo, Ph.D., Professor, Department of Mechanical Engineering and Materials Science

Thesis Advisor: Anthony J. DeArdo, Ph.D., Professor, Department of Mechanical Engineering and Materials Science

NEW OBSERVATIONS ON FLASH BAINITE

Petch Janbanjong, M.S.

University of Pittsburgh, 2016

Flash bainite is a new type of microstructure developed from new heat treatment process called "Flash Processing". Using less treatment time, the result is the high performance steel with mixed microstructure of bainite and martensite. This research aimed to study the characteristics of this process using typical low carbon steel, with 0.1-wt% C. The experiments have been done with two similar types of steels, one with vanadium and one without. Two rates of heat treatment and 3 different heating temperatures have been set up and experiments were conducted to twelve samples. The results show 2 groups of different samples, with and without bainite in the final microstructure. The samples that were heat-treated to 950 °C resulted in fractions of bainite in the end. The microstructures and characteristics of flash bainite have been studied morphologically using OM, SEM and EBSD. OM results and SEM results confirmed that the formation of bainite in flash processed steel was because of the incomplete carbides dissolution and carbon concentration gradients. SEM results showed that flash bainite samples showed characteristics of upper-bainite morphology, specifically bainitic ferrite type. EBSD results also confirmed the characteristics of bainite and the contribution to mechanical properties of the microstructures. The hardness test showed outstandingly high value in the range of 380-390 HV,

even when compared to typical bainite and martensite. The comparisons of typical flash bainite and flash bainite developed in the research have been made and concluded. Also, the comparisons between typical bainite and flash bainite have been made to confirm the type of bainite developed in this research in morphological aspect. The results showed that flash bainite could be considered as a valuable option of steels in the future. However, further experiments should be made to confirm mechanical properties of this type of steels.

TABLE OF CONTENTS

LIST OF TABLES

LIST OF FIGURES

ACKNOWLEDGEMENTS

This thesis would never be completed without encouragement and support from a lot of people in my life. First of all, I would like to express my sincere gratitude to my advisor, Prof. A. J. DeArdo, who fully supported me throughout the time of my study and who gave me countlessly advice and encouragement.

A special thanks to Dr.Goldman who tirelessly helped improving my English both grammatically and academically in my thesis writing, without him it would be difficult for me to finish the writing in a proper way.

My committee consisted of Professor Vallejo, Associate Professor Smolinski and Professor DeArdo. I appreciate their performing this task collectively and professionally. Their helpful suggestions and recommendations helped improve for different aspects for this research.

I would also like to show my gratitude to all BAMPRI members: Dr. M.J. Hua, Victoria Wang, Dr. Yu Gong, Bing Ma, Junyu Duan, Wu Yingjie and Xinchi Feng for all the support and every insightful discussions that we had together. Everybody is like my family here and without them; this thesis cannot be completed as it is.

Special acknowledgment is extended to friends from Oulu, Finland, for their kind support of heat treatment processing, I am really grateful for your help.

Most importantly, I should like to thank my family and my girlfriend for their support and encouragement throughout the tough time that I had here. Their belief and morale support

really helped me reach my goals and expectations. I would like to specifically dedicate this work to them and I hope they are proud of me. Thank you.

1.0 INTRODUCTION

Steels have played an important role in an industrial world for centuries. Various types of steels have been developed throughout these years to serve the requirements of industries. Different combinations of compositions and processing yield different characteristics of steels. Some of them have been invented to serve mechanical purposes, and some of them have been developed to serve other applications.

In the aspect of utilization, desired steels or materials have to be suitable for design requirements, or in other words, serve the purpose of usage. Mechanical properties have to be adequate to fulfill the requirements. This led to the development of various types of steels such as high strength low alloy (HSLA) steels or some mixed-microstructure steels like dual phase steels [1].

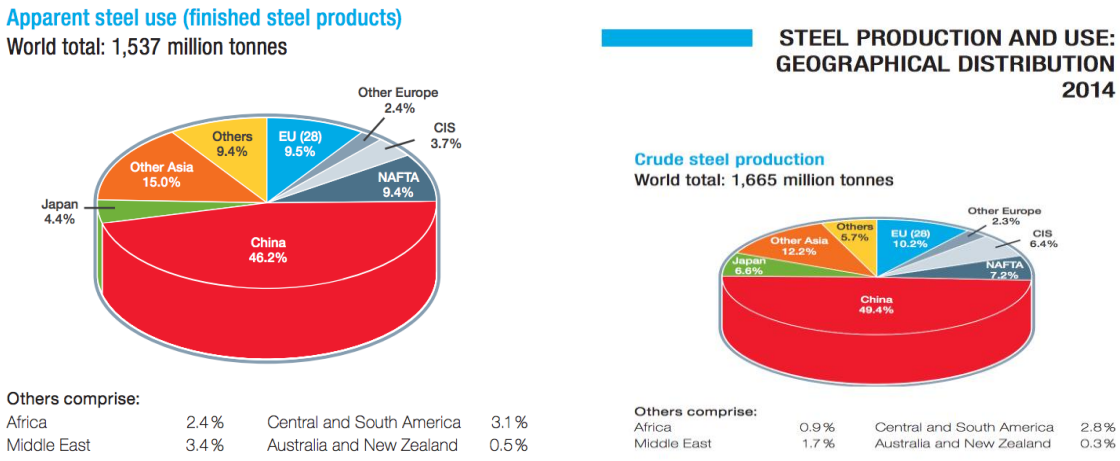

Figure 1. Steel production and use in 2014 [2]

To meet the properties requirements, microstructure characterization plays an important rol, since mechanical properties are controlled by the microstructures. Characterization and adjustment of microstructures are then, controlled by the compositions and processing of the steels. Alloying elements addition can also sometimes, control the final microstructures in the steels. So, in order to achieve the desired mechanical properties, the suitable heat treatment process has to be considered and designed.

1.1 HEAT TREATMENT

Heat treatment is a batch process of producing steels by subjecting the initial condition of steel under various time-temperature thermal cycles. The purpose of heat treatment is to adjust the characteristics of steels by means of changing microstructures. Once the steels are subjected to heat cycles, the microstructure will change according to the heating, holding time and cooling rate of the cycles. The temperature also plays an important role, since the transformation point of each phase in steels depends on compositions, time and temperatures.

Heat treatments can be controlled by several factors, which affect the final microstructures of steels. Heat treatment begins by forming austenite at temperature above the A_{c3} line. This austenite is then, cooled to room temperature in some pre-determined way. Depending on the microstructure desired, this cooling path is controlled to intersect the Continuous-Cooling-Transformations (CCT) diagram in a specific way. (Figure. 2)

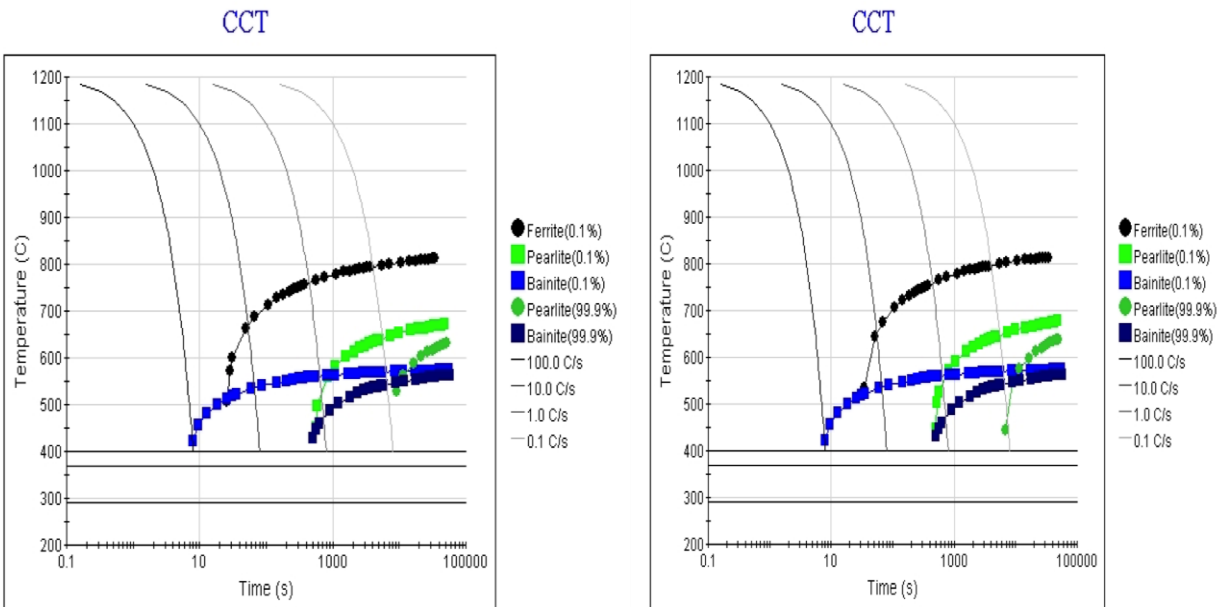

Figure 2. CCT diagram of 2A and 2B steels (Left and right**)**

By studying the CCT diagram, the heat path for the heat treatment can be designed to achieve the targeted final microstructure. However, certain heat treatments can result in long process times, which are inefficient and costly. Therefore, to avoid inefficient heat-treating; the thermal path through the CCT diagram should be reconsidered. This approach could lead to new and more efficient heat treatment processes.

1.2 FLASH PROCESS

In 2013, Cola introduced a new heat treatment process to the world called "Flash Processing" [3, 4].

Flash Processing represents a new and novel heat treatment, which uses rapid heating, short soak times and rapid cooling to achieve high performance microstructures even in simple common steels. Since Flash Processing involves simple processing, it appears that the Flash Processing maybe the next evolutionary step in the green heat treatment of steels and hence, opening up new opportunities for improvement. With less process time and less complexity, the flash process itself can save significant amount of important resources for industry. It is also claimed that Flash Processing produces new types of microstructures and properties, which are alleged to be better than those of typical microstructures [3] [4]. However, the process is still new and more details need to be discovered. This is why this research has been set up: to study details of flash process and the flash-processed steels both in morphology and properties aspect. The study aims to develop understanding of the flash process and the characteristics of steels after undergoing the process. The microstructures of the steels will be analyzed and discussed in detail about the formation of them and how important they are to the steel properties. This study will tend to broaden the understanding of Mr. Cola's process and provide more information for further study.

1.3 FLASH BAINITE

With Flash Processing, the microstructure developed is claimed to be a mixture of about 20 percent of bainite and 80 percent of martensite. The resulting steel undergoing Flash Process is called "Flash Bainite". In Cola's work, the steels used to develop flash bainite were AISI 4130 and AISI 4140, medium carbon steels. The resulting flash bainite shows properties of high strength and high ductility, opposing to martensitic microstructure steels [3, 4]. In this current

study, an HSLA steel, with and without vanadium, will be subjected to heat treatment similar to the Cola flash bainite treatment. The resulting microstructure will be evaluated using optical, scanning electron microscopy and electron backscatter diffraction. The results should provide more information on: (i) the microstructural definition and appearance of flash bainite, (ii) the conditions under which this microstructure forms and (iii) the resulting mechanical properties (hardness only).

The next step in future research could be to conduct more experiments of similar heat treatment but with different types of steels.

1.4 STATEMENT OF OBJECTIVES

As mentioned earlier, Flash Bainite is still a new field and microstructure for study. More information and principles regarding this topic still needed to be developed. This research has been set up to serve those purposes and fulfill the missing information for any further study. To summarize, the objectives of this research are:

1. To develop more understanding and information on Flash Process
2. To study and explain how Flash Bainite forms in the microstructure
3. To observe the characteristics of Flash Bainite and its microstructures
4. To explain, describe and differentiate the behavior of Flash Bainite
5. To provide more background and principles about Flash Bainite for future study and for further utilization in the steel industry

2.0 BACKGROUND

To understand flash processed bainite, the basic knowledge of the microstructures of bainite and martensite must be understood. Anytime a steel is quenched from above the A_{c3} temperature, the resulting microstructures might be bainite, martensite or mixture of the two, depending on the circumstances. Figure 3 shows upper bainite in Fe-0.095C-1.63Si-2Mn-2Cr wt% steel transformed isothermally at 400 °C on the left, and microstructure of martensite transformation in Fe-31wt%Ni-0.02wt%C transformed by cooling into liquid nitrogen on the right.

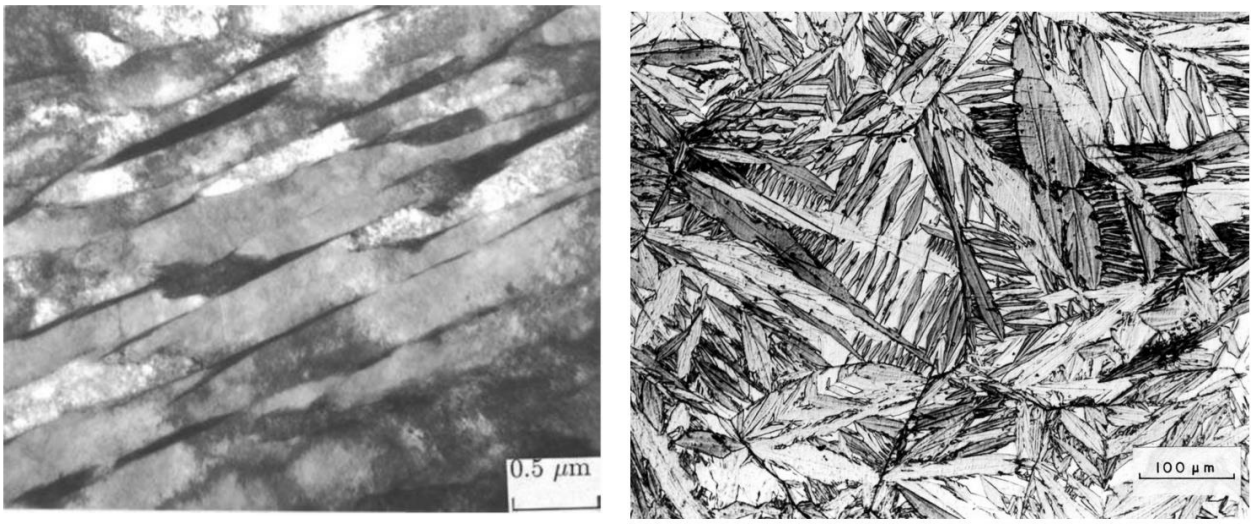

Figure 3. The microstructure of bainite (left) and martensite (right) [5, 6]

2.1 BAINITE

2.1.1 General Characteristics of Bainite

Bainite is a microconstituent since it is a non-equilibrium phase morphology, which, consists of more than one phase in the microstructure. Bainite commonly consists of dislocation-rich bainitic ferrite, plus cementite, martensite and/or retained austenite. Davenport and Bain originally described the microstructure as being similar in appearance to tempered martensite, especially in their high carbon steel [7].

Bainite has a lath or plate-like microstructure that forms in steels at temperatures of 550-250 °C, depending on alloy content [7]. First described by Davenport and Bain, it is one of the decomposition products that may form when austenite (the face centered cubic crystal structure of iron) is cooled past a critical temperature, normally around 500- 550 °C in plain carbon steels.

The temperature range for transformation to bainite (550-250 °C) is between those for pearlite and martensite. When formed during continuous cooling, the cooling rate to form bainite is more rapid than that required to form pearlite, but less rapid than is required to form martensite (in steels of the same composition). Most alloying elements will lower the temperature required for the maximum rate of formation of bainite, though carbon is the most effective in doing so [7].

The microstructures of martensite and bainite at first seem quite similar at the optical microscopic level. This is a consequence of the two microstructures sharing many aspects of their transformation mechanisms. For example, bainite is considered a displacive or shear type-reaction that is accompanied by diffusion of carbon. Martensite, on the other hand, is completely a displacive reaction, with little long-range diffusion. However, the morphological differences that do exist require a TEM to see. Under a light microscope, the microstructure of these two microconstituents can look similar.

To summarize, bainite ranks between pearlite and martensite in terms transformation temperature and hardness. For this reason, the bainitic microstructure becomes useful in that no additional heat treatments are required after initial cooling to achieve a hardness value between that of pearlitic and martensitic steels.

2.1.2 Formation of Bainite

Davenport and Bain first discussed the controversial bainite transformation theory in their work in 1930. The bainite microstructure has been discussed in the literature since that time [8]. The theory of a displacive mechanism of bainite formation by Hultgren has been proposed to explain observations of the needle-like troostite (Figure 2). Troostite was the name then, given to all fine mixtures of ferrite and cementite [7]. The first referred term was ‘martensite-troostite’ according to its morphological similarities to martensite; bainite has maintained an association with the martensitic microstructure [8]. The original micrographs of ‘martensite-troostite’ (Figure 2) revealed that the early theories of bainite formation were influenced by this mistaken identity [10, 11]. A certain amount of work has been established with the assumption that bainite is formed

with super supersaturated carbon [12, 13, 14]. One early example is the mechanism described by Vilella [15] as the rapid growth of flat plates of 'quasi-martensite' — supersaturated ferrite — which subsequently reject the excess carbon into the surrounding austenite at a rate dependent on the transformation temperature. This entire process was thought to last only a few millionths of a second. Vilella's work built upon the ideas of Davenport and Bain to form the beginnings of a diffusionless, displacive theory of transformation. Robertson also made a direct observation of the bainite microstructure prior to the 1930 paper, but failed to identify it as a new structure [16]. He compared the bainite to pearlite, suggesting that the "complete change in the crystallography of the structures" was due to pearlite being nucleated by carbide, and bainite being nucleated by ferrite. He remained convinced that the growth of the Widmanstatten-like structures was limited by carbon diffusion. Much work to follow agreed with this hypothesis and many felt that a diffusion-controlled transformation was the correct explanation [17, 18, 19, 20]. The classification of bainite into two forms — upper and lower bainite — provided an opportunity for a theory incorporating two different mechanisms of transformation. Indeed, it was suggested that upper bainite formed via a diffusion-controlled process, while lower bainite was formed via lattice shearing. Similar theories would be put forward for many years to come [17].

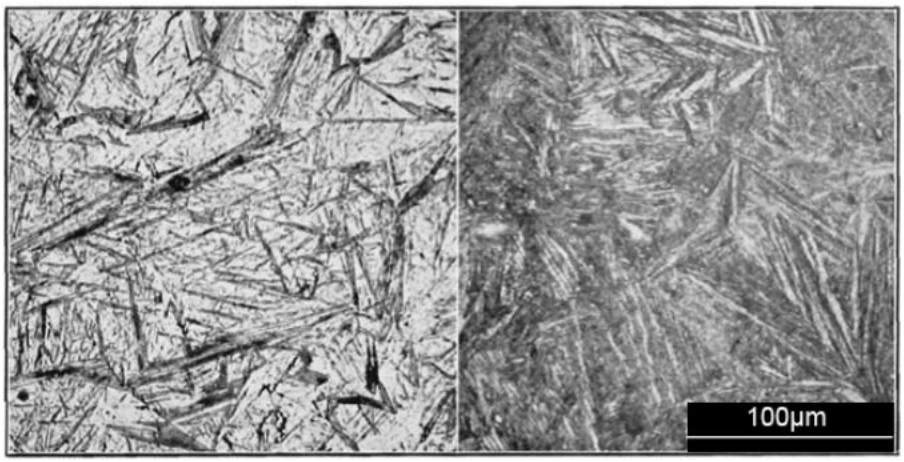

Figure 4. Martensite-troostite micrographs from Davenport and Bain [8]

At 900 °C a typical low-carbon steel is composed entirely of austenite, a high temperature phase of iron (the other being delta-ferrite at even higher temperatures). Below around 700 °C (727 °C in eutectoid iron) the austenite is thermodynamically unstable and, under equilibrium conditions, it will undergo a eutectoid reaction and form pearlite – an interleaved mixture of ferrite and cementite (Fe_3C). In addition to the thermodynamic considerations indicated by the phase diagram, the phase transformations in steel are heavily influenced by the chemical kinetics. This leads to the complexity of steel microstructures, which are strongly influenced by the cooling rate. This can be illustrated by a continuous cooling transformation (CCT) diagram which plots the time required to form a phase when a sample is cooled at a specific rate thus showing regions in time-temperature space from which the expected phase fractions can be deduced for a given thermal cycle (Figure 5) [20, 21].

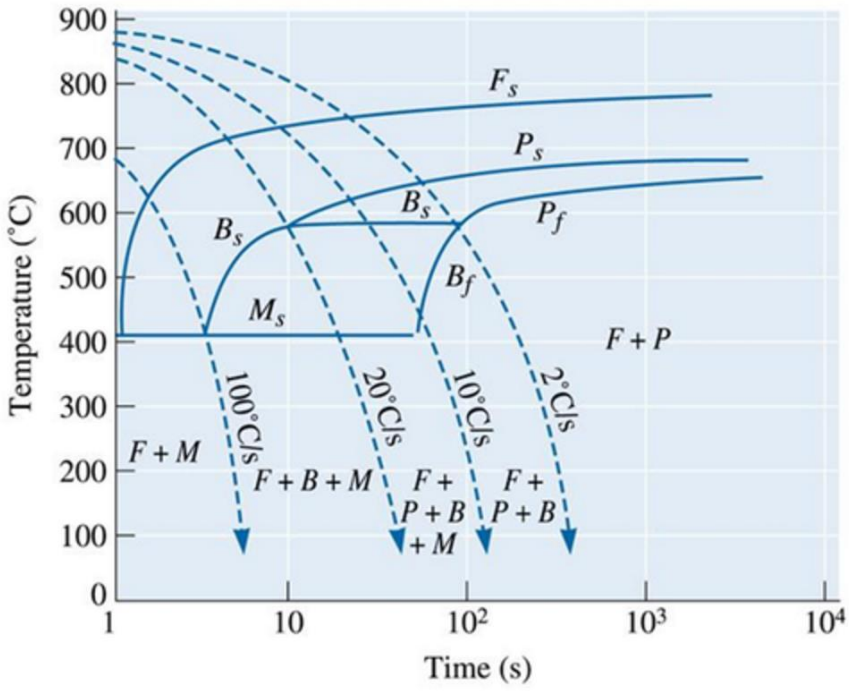

Figure 5. Continuous Cooling Transformation (CCT) diagram for eutectoid steel [20]

If the steel is cooled slowly the transformation will agree with the equilibrium predictions and pro-eutectoid ferrite will dominate the microstructure with some fraction of pearlite or cementite depending on the chemical composition. However, the transformation from austenite to pearlite is a time-dependent reconstructive reaction, which requires the large-scale movement of the iron and carbon atoms. While the interstitial carbon diffuses readily even at moderate temperatures the self-diffusion of iron becomes extremely slow at temperatures below 600 °C until, for all practical purposes, it stops. As a consequence, rapidly cooled steel may reach a temperature where pearlite can no longer form despite the reaction being incomplete and the remaining austenite being thermodynamically unstable. Austenite that is cooled very rapidly can form martensite, without any diffusion of either iron or carbon, by the shear of the austenite's face-centered crystal structure into a distorted body-centered tetragonal structure. This non-equilibrium phase can only form at low temperatures, where the driving force for the reaction is sufficient to overcome the considerable lattice strain imposed by the transformation. The transformation is essentially time-independent with the phase fraction depending only the degree of cooling below the critical martensite start temperature [20]. Further, it occurs without the diffusion of either substitutional or interstitial atoms and so martensite inherits the composition of the parent austenite.

Bainite occupies a region between these two processes in a temperature range where iron self-diffusion is limited but there is insufficient driving force to form martensite. In contrast to pearlite, where the ferrite and cementite grow cooperatively, bainite forms by the transformation of carbon-supersaturated ferrite with the subsequent diffusion of carbon and the precipitation of carbides. A further distinction is often made between so-called lower-bainite, which forms at temperatures closer to the martensite start temperature, and upper-bainite, which forms at higher

temperatures. This distinction arises from the diffusion rates of carbon at the temperature at which the bainite is forming. If the temperature is high then the carbon will diffuse rapidly away from the newly formed ferrite and form carbides in the carbon-enriched residual austenite between the ferritic plates leaving them carbide-free. At low temperatures the carbon will diffuse more sluggishly and may precipitate before it can leave the bainitic ferrite. There is some controversy over the specifics of bainite's transformation mechanism. Both theories are presented below.

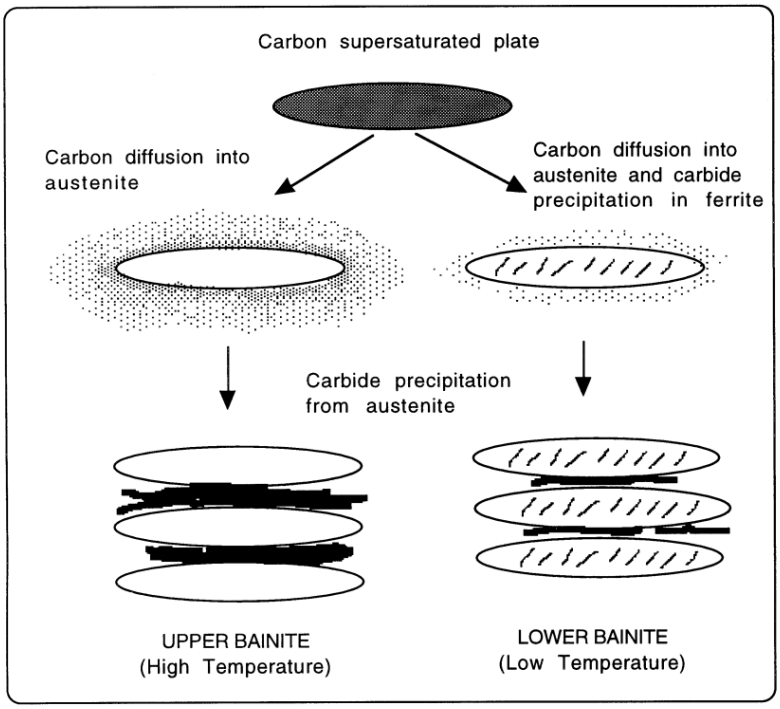

Figure 6. Simple diagram of the mechanism of bainite transformation [21]

Displacive Theory

One of the theories on the specific formation mechanism for bainite is that it occurs by a shear transformation, as in martensite. The transformation is said to cause a stress-relieving

effect, which is confirmed by the orientation relationships present in bainitic microstructures. There are, however, similar stress-relief effects seen in transformations that are not considered to be martensitic in nature, but the term 'similar' does not imply identical. The relief associated with bainite is an invariant—plane strain with a large shear component. The only diffusion that occurs by this theory is during the formation of the carbide phase (usually cementite) between the ferrite plates [22].

Diffusive Theory

The diffusive theory of bainite's transformation process is based on short-range diffusion at the transformation front. Here, random and uncoordinated thermally activated atomic jumps control formation and the interface is then rebuilt by reconstructive diffusion. The mechanism is not able to explain either the shape or surface relief caused by the bainite transformation [22].

2.1.3 Kinetics of transformation

There are three distinct events in the evolution of bainite (Figure 5). A sub-unit nucleates at an austenite grain boundary and lengthens until its growth is arrested by plastic deformation within the austenite. New sub-units then nucleate at its tip, and the sheaf structure develops as this process continues. The average lengthening rate of a sheaf must be smaller than that of a sub-unit because of the delay between successive sub-units. The volume fraction of bainite depends on the totality of sheaves growing from different regions in the sample. Carbide precipitation influences the reaction rate by removing carbon either from the residual austenite or from the supersaturated ferrite [21].

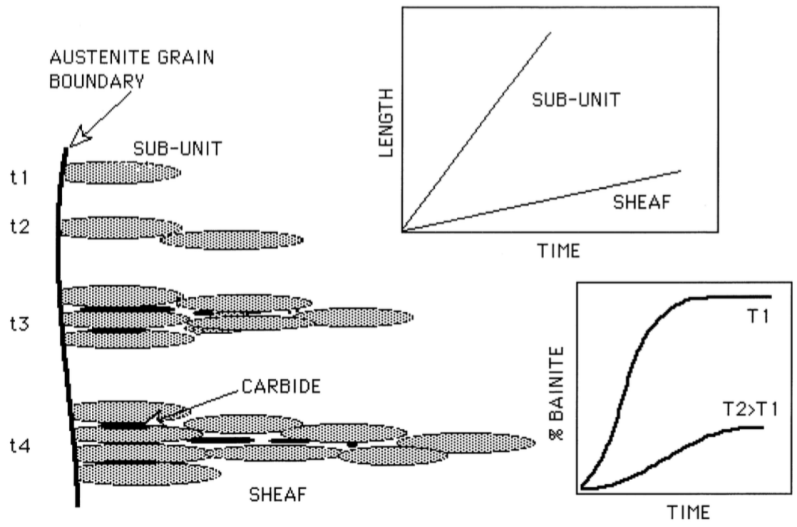

Figure 7. Evolution of bainite [21]

Ferrite crystals nucleate from the austenite grain boundaries and lengthen until its growth is arrested by plastic deformation within the austenite. Carbon will be rejected from ferrite to austenite. New ferrite sub-unit nucleates at the end of the ferrite crystal tip. The sheaf structure develops as this process continues. Carbide precipitation influences the reaction rate by removing carbon either from the residual austenite or from the supersaturated ferrite.

Austenite conditioning can affect the diagram. Austenite conditioning increases the Sv offering more nucleation sites. This leads to an increase in nucleation. As a result, the upper nose will be moved toward shorter times. To avoid the nucleation of the pearlite at high temperature, alloying or rapid cooling will be required [21].

It is a common observation that the Widmanstatten ferrite-start (W_S) and bainite-start (B_S) temperatures are more sensitive to the steel composition than is the Ae_3 temperature. This indicates that the influence of solutes on the nucleation of Widmanstatten ferrite and bainite is more than just thermodynamic.

Some clues to this behavior come from studies of time-temperature-transformation diagrams, which consist essentially of two C-curves. The lower C- curve has a characteristic flat top at a temperature, T_h, which is the highest temperature at which ferrite can form by displacive transformation. The transformation product at T_h may be Widmanstatten ferrite or bainite.

The temperature range for the transformation to bainite (250–550 °C) is between those for pearlite and martensite. It can be demonstrated for many steels that there is a temperature, B_S, above which no bainite will form. In some steels, this corresponds to the bay in the TTT diagram between the overlapping curves of pearlite and bainite. This temperature is well below that at which pro-eutectoid ferrite formation becomes thermodynamically possible [23].

2.1.4 Metallographic Structure

Although upper bainite and lower bainite are two general forms of bainite often found in most engineering steels, several other types of bainite are observed according to its morphologies. The mechanical properties vary depending on the bainite morphologies. Since bainite microstructures are complex, several definitions describing bainite microstructure are used. Thus, a short review of these definitions is necessary.

Upper Bainite:

So-called "upper bainite" forms around 400–550 °C in sheaves. These sheaves contain several laths of ferrite that are approximately parallel to each other and which exhibit a Kurdjumov-Sachs relationship with the surrounding austenite, though this relationship degrades

as the transformation temperature is lowered. The ferrite in these sheaves has a carbon concentration below 0.03 percent, resulting in carbon-rich austenite around the laths.

The amount of cementite that forms between the laths is based on the carbon content of the steel. For low carbon steel, typically discontinuous "stringers" or small particles of cementite will be present between laths. For higher carbon steel, the stringers become continuous along the length of the adjacent laths [7, 21, 22]

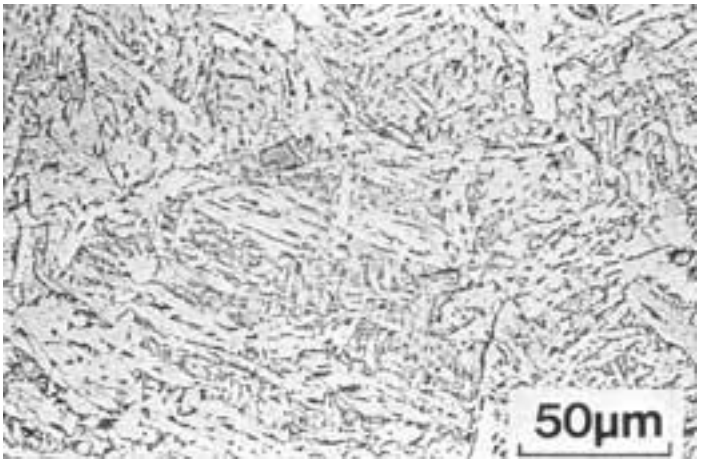

Figure 8. Upper bainite structure [22]

Lower Bainite:

Lower bainite forms between 250 and 400 °C and takes a more plate-like form than upper bainite. There are not nearly as many low angle boundaries between laths in lower bainite. In lower bainite, the habit plane in ferrite will also shift from <111> towards <110> as transformation temperature decreases. In lower bainite, cementite nucleates on the interface between ferrite and austenite [21].

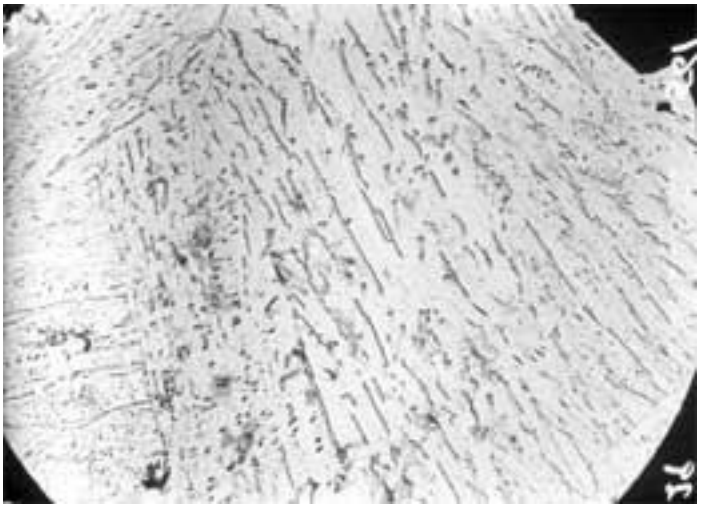

Figure 9. Lower bainite structure [21]

Granular Bainite

Granular bainite is a term frequently used to describe the bainite that occurs during continuous cooling transformation. This terminology is used widely in industry, where most steels undergo non-isothermal heat treatments. A good example is the energy generation industry where large Cr-Mo steel components are allowed to cool naturally from the austenitic state and create bainitic microstructures.

In the case of medium and high carbon content steels, granular bainite cannot readily be distinguished from ordinary bainite when examined using transmission electron microscopy, because its mechanism of formation is not different. However, because the microstructure forms gradually during cooling, the sheaves of bainite can be rather coarse. The optical microstructure then gives the appearance of blocks of bainite and austenite; hence it is called “granular bainite”.

A characteristic feature of granular bainite is the lack of carbides in the microstructure. Instead, the carbon that is partitioned from the bainitic ferrite stabilises the residual austenite, so that the final microstructure contains both retained austenite and some high carbon martensite in addition to the bainitic ferrite [21, 22].

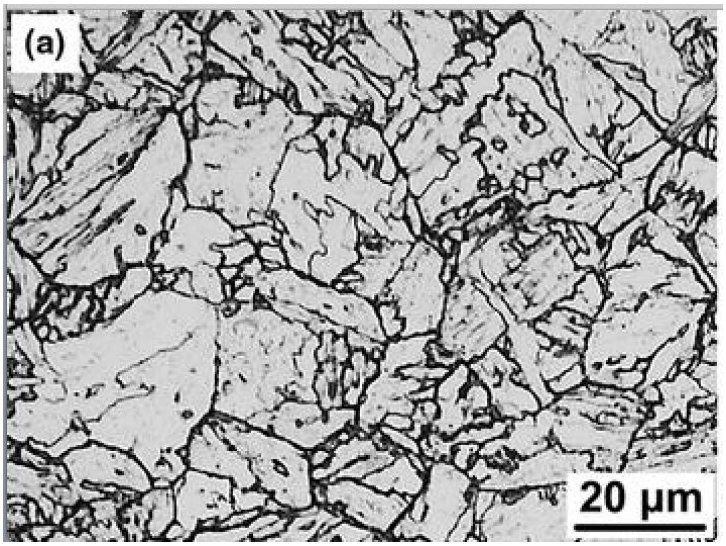

Figure 10. Granular bainite structure [21]

Bainitic Ferrite

Both upper and lower bainite consist of aggregates of plates of ferrite, separated by untransformed austenite, martensite or cementite. The aggregates of plates are called sheaves and the plates within each sheaf are the sub-units. The sub-units are not isolated from each other but are connected in three dimensions. The shape of a sheaf is that of wedge-shaped plate. The thicker end of the wedge begins at the nucleation site, which is usually an austenite grain surface. The sub-units, which make up the sheaf, have a lenticular plate or lath morphology, whose form is most prominent near the edge or tip of a sheaf where impingement effects are minimal. When

the sub-units are in the form of laths, they are longest along the close packed direction of the ferrite, which is mostly parallel to a corresponding close packed direction of the austenite [7, 22].

Zajac et al., classified bainite in a different way, based on the morphologies of ferrite and the type of second phase in the microstructure. Five types of bainite can be classified using this basis: granular bainite, upper bainite, degenerate upper bainite, lower bainite and degenerate lower bainite. The descriptions of each type are as followed [24].

Granular bainite: A characteristic (though not unique) feature of granular bainite is the lack of carbides in the microstructure. The carbon that is partitioned from the bainitic ferrite stabilizes the residual austenite, so that the final microstructure contains both retained austenite and some high-carbon martensite along with the bainitic ferrite.

Upper bainite: ferritic laths with some carbides in between.

Degenerate upper bainite: In some steels, the cementite formation is prevented, and the microstructure is composed of ferritic lath with thin layers of retained austenite or martensite in between laths.

Lower bainite: carbides precipitate inside ferrite.

Degenerate lower bainite: carbides are prevented to form, and the retained austenite instead of carbides precipitate inside the ferrite.

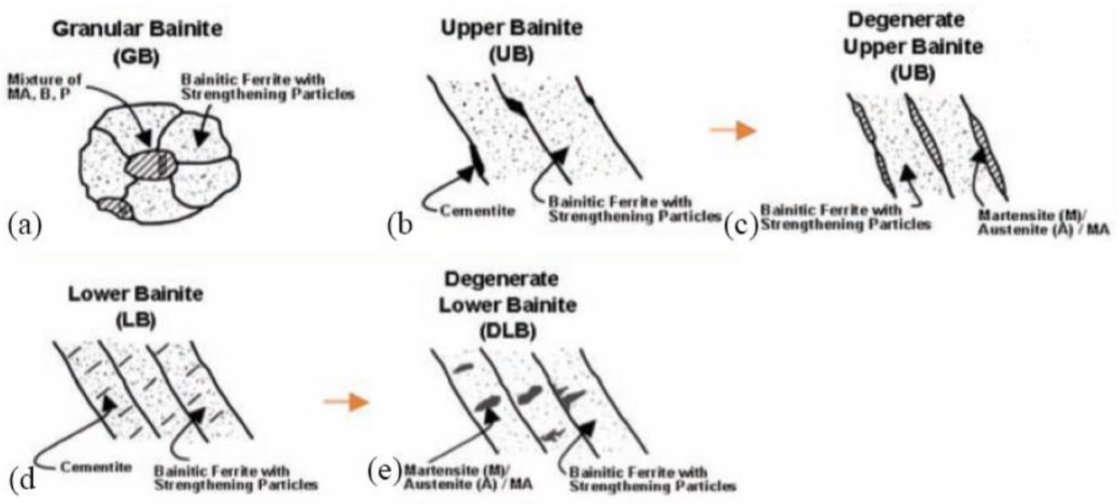

Figure 11. Bainite classification on the basis of ferrite morphologies and types of second phase [24]

2.1.5 Hardness

The hardness of bainite increases linearly with carbon concentration, by approximately 190 HV per w% C. This contrasts with a change of about 950 HV per weight percent in the case of carbon-supersaturated martensite. The austenitising temperature does not influence the hardness unless it is not high enough to dissolve all the carbides. For mixed microstructures, the hardness depends on the transformation temperature and composition. This is because the stability of the residual austenite to martensitic transformation changes with its carbon concentration, the limiting value of which depends on the transformation temperature via the T_0 curve of the phase diagram.

Reconstructive transformations become incredibly slow below B_S in high- alloy steels. Hence, any austenite left untransformed during the bainitic reaction either decomposes into untempered high-carbon martensite or is retained to ambient temperature. In low-alloy steels the

residual austenite may transform into some form of degenerate pearlite. These secondary transformations have for a long time been known to influence the hardness of the microstructure. Lyman and Troiano [25] found that for a series of Fe-Cr-C alloys the hardness for the 0.08 weight percent C alloy was insensitive to the isothermal transformation temperature. The low carbon concentration ensures that the microstructure is almost fully bainitic for all of the temperatures studied. This contrasts with higher carbon alloys, where the hardness first decreases as the transformation temperature is reduced because the fraction of bainite increases at the expense of residual phases like martensite and degenerate pearlite [25].

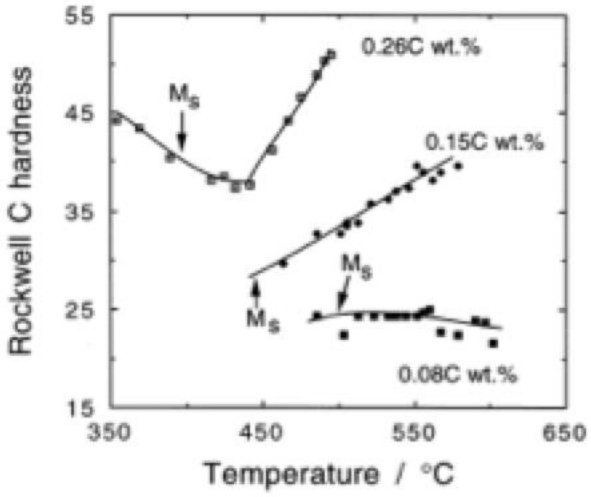

Figure 12. Variation of hardness as a function of isothermal transformation temperature [25]

The micro hardness of bainite in a mixed microstructure of bainite and pearlite obtained by isothermal transformation is less than that of the pearlite. This remains the case even when the pearlite and bainite have been generated at the same temperature. This behavior is easy to explain once it is realized that the pearlite grows from carbon-enriched austenite and hence contains a much larger fraction of cementite than the bainite.

In the case of medium and high carbon contents, the hardness of bainite is insensitive to the austenite grain size even though the latter influences the bainite sheave thickness [26]. This is expected since the bainite sub-unit size is hardly influenced by the austenite grain size. Since the sub-units are much smaller they exert an overriding influence on strength. For the same reason, the hardness of fully bainitic microstructures is not sensitive to the austenitising temperature [26, 27].

The hardness of bainite increases linearly with carbon concentration by approximately 190 HV per weight percent. Vicker hardness can be converted to tensile strength: therefore, with high carbon will result in higher strength [28].

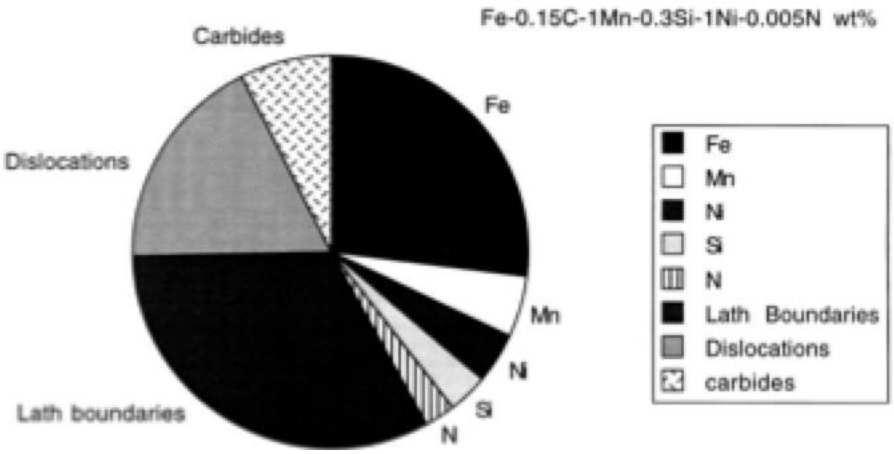

Figure 13. Estimated contributions to the strength of a fully bainitic sample [28]

2.2 MARTENSITE

2.2.1 General Characteristics of Martensite

Martensite, named after the German metallurgist Adolf Martens (1850–1914), most commonly refers to a very hard form of steel crystalline structure, but it can also refer to any crystal structure that is formed by diffusionless transformation. It includes a class of hard minerals occurring as lath- or plate-shaped crystal grains. When viewed in cross section, the lenticular (lens-shaped) crystal grains are sometimes, incorrectly, described as acicular (needle-shaped) [29].

It was used originally to describe the hard microconstituent found in quenched steels. Martensite remains of the greatest technological importance in steels where it can confer an outstanding combination of strength (> 3500 MPa) and toughness (> 200 MPa $m^{1/2}$). Many materials other than steel are now known to exhibit the same type of solid-state phase transformation, known as a martensitic transformation, frequently also called a shear or displacive transformation. Martensite occurs in, for example, nonferrous alloys, pure metals, ceramics, minerals, inorganic compounds, solidified gases and polymers (Table 1) [30].

Table 1. The temperature MS at which martensite first forms on cooling, and the approximate Vickers hardness of the resulting martensite for a number of materials [30]

Composition	M_S/K	Hardness, HV
ZrO_2	1200	1000
Fe–31Ni–0.23C weight percent	83	300
Fe–34Ni–0.22C weight percent	<4	250
Fe–3Mn–2Si–0.4C weight percent	493	600
Cu–15Al	253	200
Ar–40N_2	30	

Martensite is a body-centered tetragonal form of iron in which some carbon is dissolved. Martensite forms during quenching, when the face centered cubic lattice of austenite is distorted into the body centered tetragonal structure without the loss of its contained carbon atoms into cementite and ferrite. Instead, the carbon is retained in the iron crystal structure, which is stretched slightly so that it is no longer cubic. Martensite is more or less ferrite supersaturated with carbon. Figure 14 shows the microstructure of typical martensite.

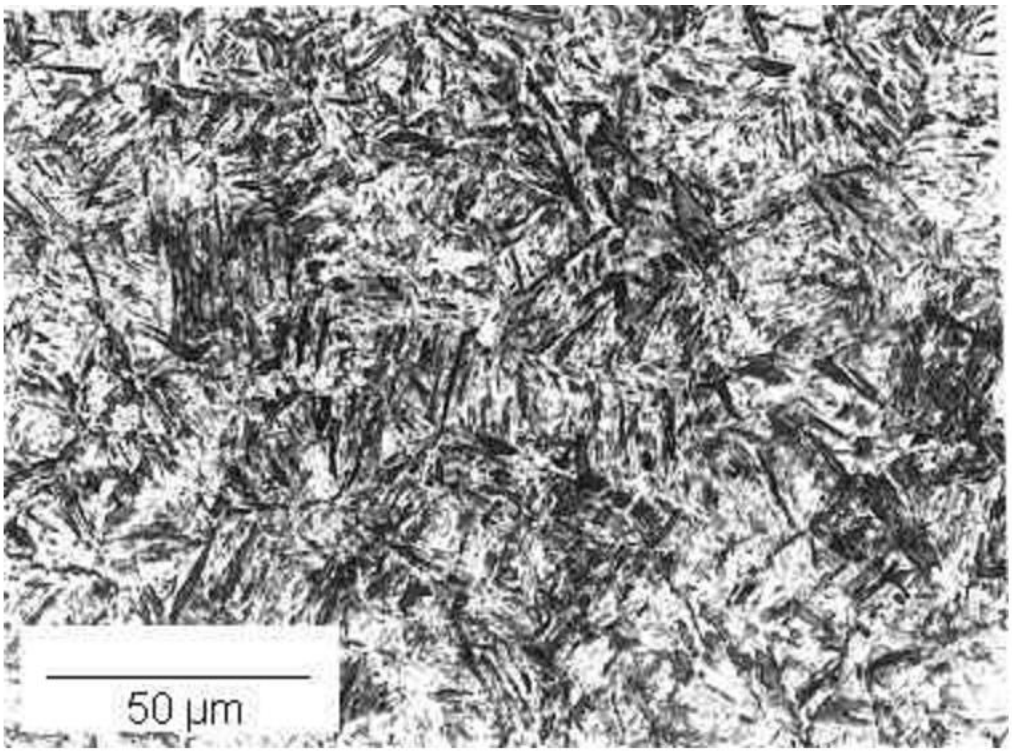

Figure 14. Photomicrograph of martensitic microstructure [31]

One of the differences between the two phases (martensite and austenite), is that martensite has a body-centered tetragonal (BCT) crystal structure, whereas austenite has a face-centered cubic (FCC) structure. The transition between these two structures requires very little thermal activation energy because it is a diffusionless transformation, which results in the subtle but rapid rearrangement of atomic positions, and has been known to occur even at cryogenic temperatures [29]. Martensite has a lower density than austenite, so that the martensitic transformation results in a relative change of volume [32]. Of considerably greater importance than the volume change is the shear strain, which has a magnitude of about 0.26 and which determines the shape of the plates of martensite [31].

Martensite is not shown in the equilibrium phase diagram of the iron-carbon system because it is not an equilibrium phase. Equilibrium phases form by slow cooling rates that allow

sufficient time for diffusion, whereas martensite is usually formed by very high cooling rates. Since chemical processes (the attainment of equilibrium) accelerate at higher temperature, martensite is easily destroyed by the application of heat. This process is called tempering. In some alloys, the effect is reduced by adding elements such as tungsten that interfere with cementite nucleation, but, more often than not, the phenomenon is allowed to proceed to relieve stresses. Since quenching can be difficult to control, many steels are quenched to produce an overabundance of martensite, and then tempered to gradually reduce its concentration until the right structure for the intended application is achieved. The needle-like microstructure of martensite leads to brittle behavior of the material. Too much martensite leaves steel brittle, too little leaves it soft [32, 33].

2.2.2 Formation of Martensite

Martensite is formed in carbon steels by the rapid cooling (quenching) of austenite at such a high rate that carbon atoms do not have time to diffuse out of the crystal structure in large enough quantities to form cementite (Fe_3C). As a result, the face-centered cubic austenite transforms to a highly strained body-centered tetragonal form of ferrite that is supersaturated with carbon. The shear deformations that result produce large numbers of dislocations, which is a primary strengthening mechanism of steels. The highest hardness of pearlitic steel is 400 Brinell whereas martensite can achieve 700 Brinell. The martensitic reaction begins during cooling when the austenite reaches the martensite start temperature (M_s) and the parent austenite becomes mechanically unstable. As the sample is quenched, an increasingly large percentage of the austenite transforms to martensite until the lower transformation temperature, M_f, is reached, at which time the transformation is completed [29]. For a eutectoid

steel, between 6 and 10percent of austenite, called retained austenite, will remain. The percentage of retained austenite increases from insignificant for less than 0.6 percent C to 13 percent retained austenite at 0.95 percent C and 30–47 percent retained austenite for a 1.4percent carbon steels. A very rapid quench is essential to create martensite. For a eutectoid carbon steel (0.78 percent C) of thin section, if the quench starting at 750 °C and ending at 450 °C takes place in 0.7 seconds (a rate of 430 °C/s) no pearlite will form and the steel will be martensitic with small amounts of retained austenite [29, 34].

Rapid quenching of austenite to room temperature often results in the formation of martensite, a very hard structure in which the carbon, formerly in solid solution in the austenite, remains in solution in the new phase. Unlike ferrite or pearlite, martensite forms by a sudden shear process in the austenite lattice, which is not normally accompanied by atomic diffusion.

Ideally, the martensite reaction is a diffusionless shear transformation, highly crystallographic in character, which leads to a characteristic lath or lenticular microstructure. The martensite reaction in steels is the best known of a large group of transformations in alloys in which the transformation occurs by shear without change in chemical composition. The generic name of martensitic transformation describes all such reactions [35].

It should however be mentioned that there is a large number of transformations which possess the geometric and crystallographic features of martensitic transformations, but which also involve diffusion. Consequently, the broader term of shear transformation is perhaps best used to describe the whole range of possible transformations [32, 35].

The martensite reaction in steels normally occurs athermally, i.e. during cooling in a temperature range, which can be precisely defined for particular steel. The reaction begins at a martensitic start temperature, M_s, which can vary over a wide temperature range from as high

as 500°C to well below room temperature, depending on the concentration of γ-stabilizing alloying elements in the steel [33].

Once the M_s is reached, further transformation takes place during cooling until the reaction ceases at the M_f temperature. At this temperature, all the austenite should have transformed to martensite but frequently, in practice, a small proportion of the austenite does not transform. Larger volume fractions of austenite are retained in some highly alloyed steels, where the M_f temperature is well below room temperature.

To obtain the martensitic reaction it is usually necessary for the steel to be rapidly cooled, so that the metastable austenite reaches M_s, the rate of cooling must be sufficient to suppress the higher temperature diffusion-controlled ferrite and pearlite reactions, as well as other intermediate reactions such as the formation of bainite. The critical rate of cooling required is very sensitive to the alloying elements present in the steel and, in general, will be lower the higher total alloy concentration [33].

Each grain of austenite transforms by the sudden formation of thin plates or laths of martensite of striking crystallographic character. The laths have a well-defined habit plane and they normally occur on several variants of this plane within each grain. The habit plane is not constant, but changes as the carbon content is increased [32, 34].

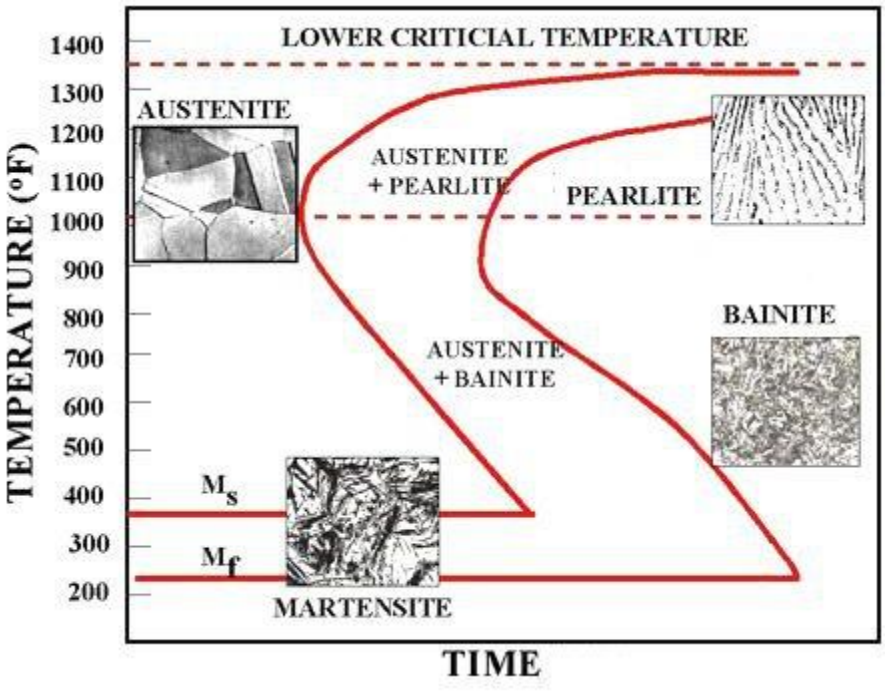

Figure 15. Illustration of Ms and Mf temperature on TTT diagram for eutectoid steel [28]

2.2.2 Microstructures of Martensite

Martensite microstructures, in modern discussions, can be described using 3 important terms: lath, packets and blocks. Lath martensite in steel is well known to show a hierarchical microstructure consisting of packets, blocks, sub-blocks, and laths. The prior austenite grain is divided into packets that consist of blocks. These blocks in a packet have the same habit plane. The packet is further divided into plate-like blocks, which consist of laths with a similar crystal orientation. Recently, it has been recognized that a block contains components called sub-blocks, each of which corresponds to a single variant characterized by the

Kurdjumov–Sachs (K–S) orientation relationship with austenite [34, 36]. Further discussion will be presented below.

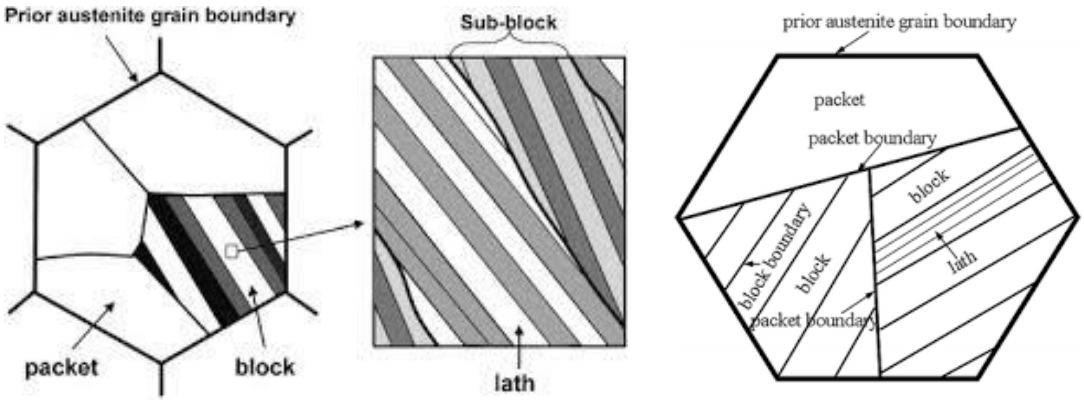

Figure 16. Schematic illustration of martensite microstructures [36]

Lath Martensite/ Low Carbon Martensite

This type of martensite is found in plain carbon and low alloy steels up to about 0.5-weight percent carbon. The morphology is lath or plate-like, where the laths are very long. These are grouped together in packets with low angle boundaries between each lath, although a minority of laths is separated by high angle boundaries. In plain carbon steels practically no twin-related laths have been detected [34, 36].

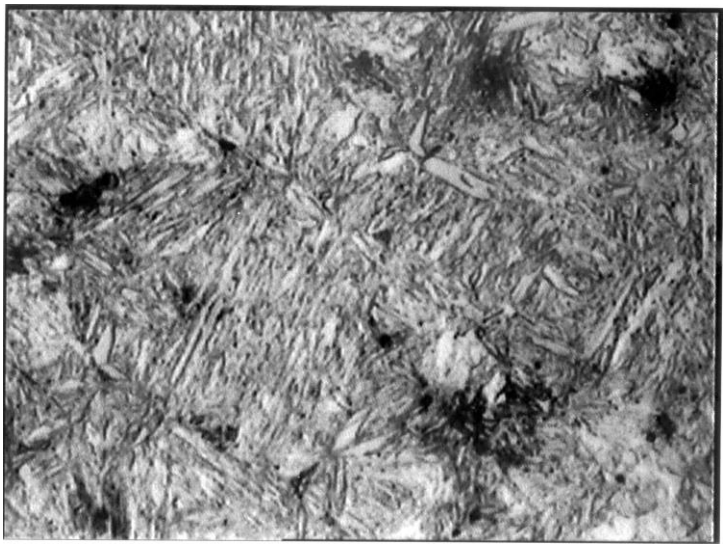

Figure 17. Lath martensite microstructure, 0.35 percent carbon-steel, water-quenched from 870 °C [29]

Plate Martensite/ Medium-High Carbon Martensite

For steel greater than 1percent carbon it will form a plate like structure called plate martensite. Between those two percentages, the physical appearance of the grains is a mix of the two. It is perhaps unfortunate that the term acicular is applied to this type of martensite because its characteristic morphology is that of perpendicular plates, a fact easily demonstrated by examination of plates intersecting two surfaces at right angles.

These plates first start to form in steels with about 0.5 wt% C, and can be concurrent with lath martensite in the range 0.5 - l.0 wt% C. Unlike the laths, the lenticular plates form in isolation rather than in packets, on planes approximating to {225} and on several variants within one small region of a grain, with the result that the structure is very complex.

The burst phenomenon probably plays an important part in propagating the transformation, and the austenite is thus not as uniformly or as efficiently eliminated as with lath martensites. This physical difference cannot be unconnected with the fact that higher percentages of retained austenite occur as the carbon level is increased, and the martensite is predominantly lenticular. The micro twinning referred to earlier is found predominantly in this type of martensite, which forms at lower M_s temperatures, as the carbon content increases.

When the carbon content is >1.4weight percent, the orientation relationship changes from Kurdjumov-Sachs to Nishiyama, and the habit plane changes to around {259}. The change is not detectable microscopically as the morphology is still lenticular plates, which form individually and are heavily twinned.

Detailed crystallographic analysis shows that this type of martensite obeys more closely the theoretical predictions than the {225} martensite. The plates are formed by the burst mechanism and often an audible click is obtained. The {259} martensite only forms at very high carbon levels in plain carbon steels, although the addition of metallic alloying elements causes it to occur at much lower carbon contents, and in the extreme case in a carbon-free alloy such as Fe-Ni when the nickel content exceeds about 29 weight percent [34, 36].

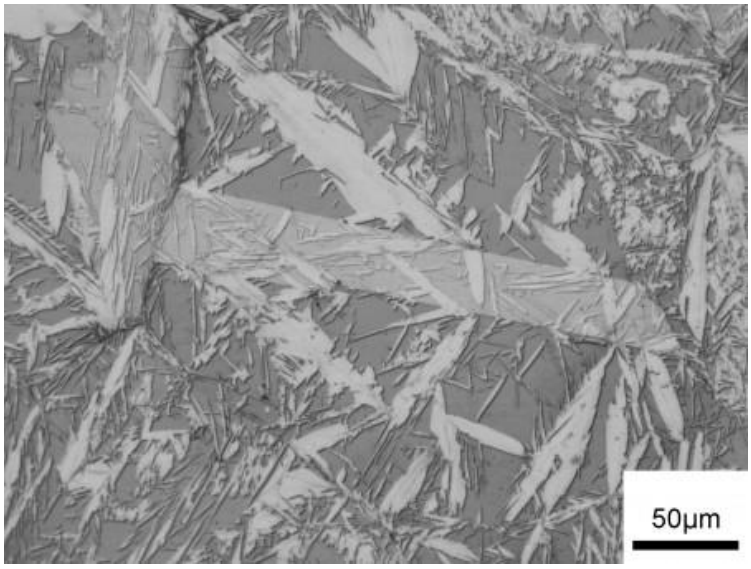

Figure 18. Light optical image of plate martensite in Fe-C [29]

2.2.3 Properties of Martensite

Martensite is a supersaturated solid solution of carbon in iron, which has a body-centered tetragonal structure, a distorted form of bcc iron. It is interesting to note that carbon in interstitial solid solution expands the fcc iron lattice uniformly, but with bcc iron the expansion is nonsymmetrical giving rise to tetragonal distortion.

Analysis of the distortion produced by carbon atoms in the several types of sites available in the fcc and bcc lattices, has shown that in the fcc structure the distortion is completely symmetrical, whereas in the bcc one, interstitial atoms in z positions will give rise to much greater expansion of iron-iron atom distances than in the x and y positions.

Assuming that the fcc-bcc tetragonal transformation occurs in a diffusionless way, there will be no opportunity for carbon atoms to move, so those interstitial sites already occupied by

carbon will be favored. Since only the z sites are common to both the fcc and bcc lattices, on transformation there are more carbon atoms at these sites causing the z-axis to expand, and the non-regular the martensite, as well as the shape deformation for a number of martensitic transformations including ferrous martensites. It is, however, necessary to have accurate data, so that the habit planes of individual martensite plates can be directly associated with a specific orientation relationship of the plate with the adjacent matrix.

Martensitic planes in steel are frequently not parallel-sided; instead they are often perpendicular as a result of constraints in the matrix, which oppose the shape change resulting from the transformation. This is one of the reasons why it is difficult to identify precisely habit planes in ferrous martensite. However, it is not responsible for the irrational planes, but rather the scatter obtained in experiments.

Another feature of higher carbon martensites is the burst phenomenon, in which one martensite plate nucleates a sequence of plates presumably as a result of stress concentrations set up when the first plate reaches an obstruction such as a grain boundary or another martensite plate.

Perhaps the most striking advances in the structure of ferrous martensites occurred when thin foil electron microscopy was first used on this problem. The two modes of plastic deformation are needed for the inhomogeneous deformation part of the transformation, i.e. slip and twinning. All ferrous martensites show very high dislocation densities of the order of 10^{11} to $10^{12}cm^2$, which are similar to those of very heavily cold-worked alloys. Thus it is usually impossible to analyze systematically the planes on which the dislocations occur or determine their Burgers vectors.

The lower carbon (<0.5 wt% C) martensites on the whole exhibit only dislocations. At higher carbon levels, very fine twins (5-10 nm wide) commonly occur. In favorable circumstances, the twins can be observed in the optical microscope, but the electron microscope allows the precise identification of twins by the use of the selected area electron diffraction technique. Thus, the twin shears can be analyzed precisely and have provided good evidence for the correctness of the crystallographic theories discussed above. However, twinning is not always fully developed and even within one plate some areas are often untwined. The phenomenon is sensitive to composition.

The evidence suggests that deformation by dislocations and by twinning are alternative methods by which the lattice invariant deformation occurs. From general knowledge of the two deformation processes, the critical resolved shear stress for twinning is always much higher than that for slip on the usual slip plane. This applies to numerous alloys of different crystal structure. Thus, it might be expected that those factors, which raise the yield stress of the austenite, and martensite, will increase the likelihood of twinning. The important variables are:

- Carbon concentration;
- Alloying element concentration;
- Temperature of transformation;
- Strain rate.

The yield stress of both austenite and martensite increases with carbon content, so it would normally be expected that twinning would, therefore, be encouraged. Likewise, an increase in the substitutional solute concentration raises the strength and should also increase the incidence of twinning, even in the absence of carbon, which would account for the twins observed in

martensite in high concentration binary alloys such as Fe-32%Ni. A decrease in transformation temperature, i.e., reduction in M_s, should also help the formation of twins, and one would particularly expect this in alloys transformed, for example, well below room temperature.

It should also be noted that carbon concentration and alloying element concentration should assist by lowering M_s. As martensite forms over a range of temperatures, it might be expected in some steels that the first formed plates would be free of twins whereas the plates formed nearer to M_s would more likely be twinned.

However, often plates have a mid-rib along which twinning occurs, the outer regions of the plate being twin-free. This could possibly take place when the M_s is below room temperature leading to twinned plates, which might then grow further on resting at room temperature.

Also, the grain angle boundary plays important role on mechanical characteristics of martensite. Both the low angle and high angle grain boundaries can increase the strength by grain boundary strengthening. However, only the high angle grain boundaries can increase the toughness by stopping the growth of cleavage crack causing catastrophic failure [32, 34, 36].

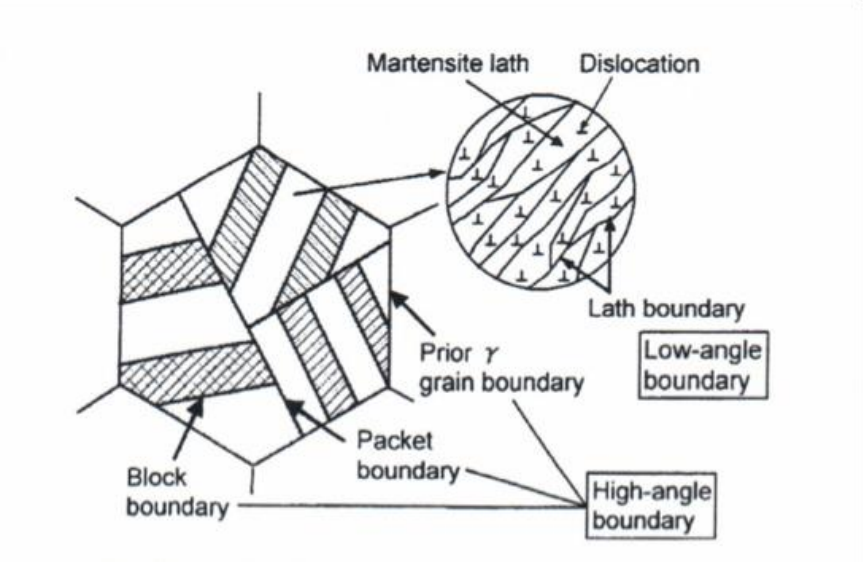

Figure 19. HAGB contributes to increasing toughness [27]

2.3 FLASH BAINITE

2.3.1 The General Idea of Flash Processing

Flash processing [FP] is an innovative steel heat treatment based on the concept of rapid thermal cycling to create a mixed microstructure consisting of martensite, bainite, and carbides. Initially, the experiment was performed using market-grade AISI 4140 steel (0.4 %C, 1.1 %Cr and 1% Mn). The test was aimed to obtain data of mechanical properties and final morphology of specimens. It is generally understood that the ductility of a material decreases as strength increases [3].

However, the unique microstructure produced by FP results in extremely high strength steel while maintaining high ductility for the given strength. These properties vary for different alloys; reaching an ultimate tensile strength (UTS) of 1.99 GPa [288.6 ksi] while maintaining 10.2 percent total elongation for flash processed AISI 4140. The result showed that the UTS value was outstandingly high, even compared to martensitic steel of the same composition. This called for detailed study of the microstructure and transformation process during the heat treatment for more understanding and broader usage of this process in the future [3].

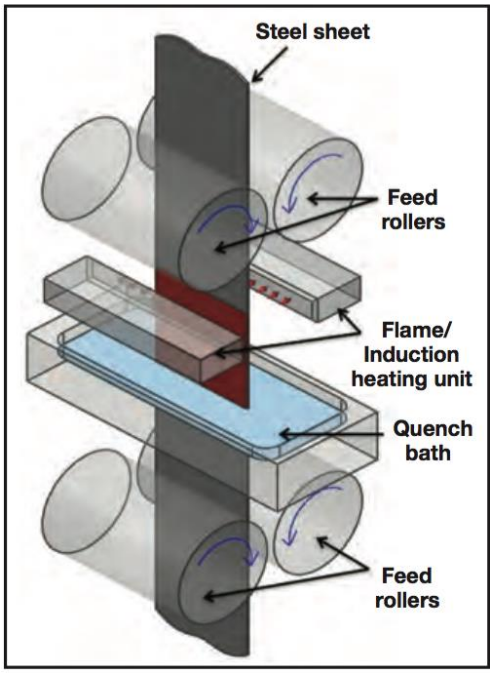

Figure 20. Schematic diagram of flash processing [4]

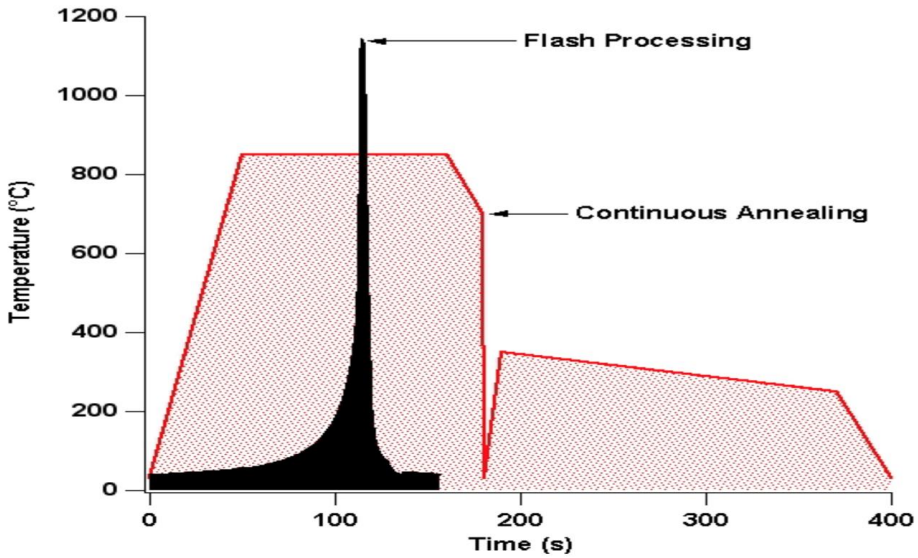

Figure 21. Schematic diagram of flash heat treatment compared to typical annealing [4]

2.3.2 Formation of Flash Bainite

Flash-processed microstructures depend on the initial microstructure, steel composition and non-equilibrium conditions resulting from high heating rates, short hold times, and high cooling rates. A schematic of the microstructural evolution during different stages is shown in Figure 22 [4].

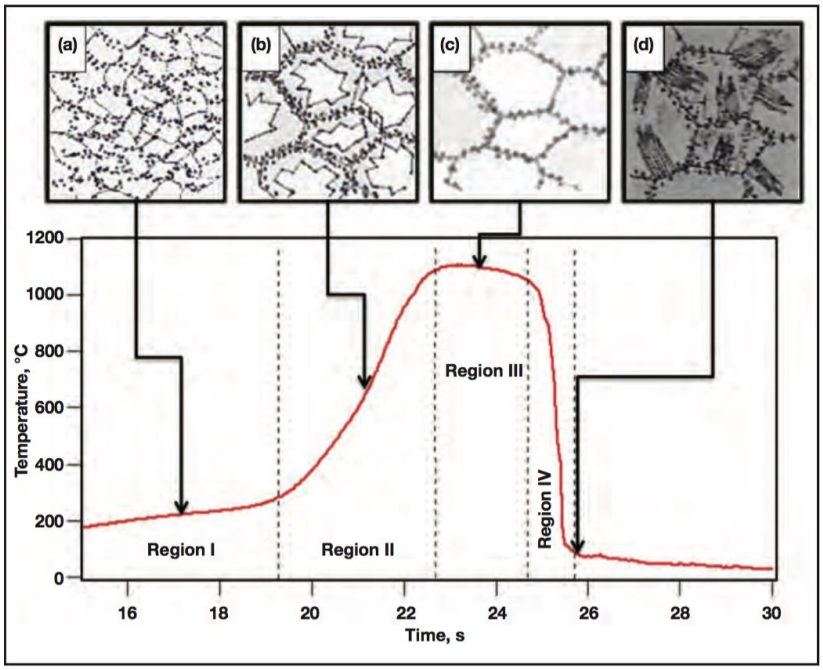

Figure 22. Schematic of microstructure evolution during the process [4]

Stage I: Initial condition before rapid heating

The microstructure should better be enriched with chromium carbides along with ferrite carbide grains: $(Fe,Cr)_3C$. This will lead to slow dissolution of carbides and it is important for the carbides to remain during the process [4].

Stage II: Rapid heating above Ac_3

The rapid heating causes austenite to start nucleation and consumes ferrite grains. The A_3 temperature will exceed the equilibrium value and the peak temperature will be above the non-equilibrium A_{c3} transformation temperature [4].

Stage III: Holding period at peak temperature

The short period of holding time results in austenite grains to completely consume ferrite grains and then start to dissolve carbides. However, carbides will not be completely dissolved due to chromium in the composition. Chromium acts as an inactive agent for carbides dissolution in this case. Moreover, the short holding time is not sufficient for carbon to fully dissolve into austenite grains and this will result in carbon concentration gradients: austenite with regions of high carbon near partially dissolve carbides and regions of low carbon far from the carbides [4].

Stage IV: Rapid quenching

The specimen will be rapidly quenched after a short holding period. The regions of high carbon will transform into martensitic microstructures, whereas the regions with low carbon will transform into bainitic microstructure. Martensite acts as a strengthening agent and bainite provides more ductility to the steel. The result would be the combination of high strength and high ductility steel [4].

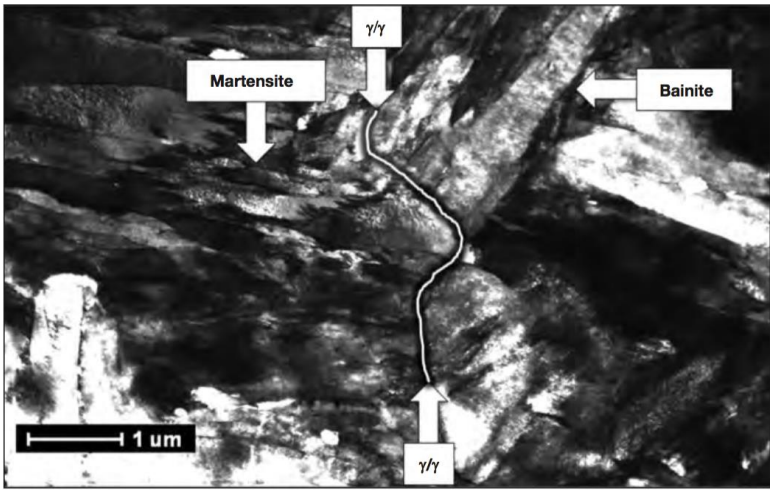

Figure 23. TEM micrograph of flash bainite microstructure [3, 4]

This process creates the formation of small, bainitic plates within a matrix of martensite. The rapid heating during the process results in a heterogeneous distribution of carbon within the austenite phase. Upon quenching, the austenite decomposes to a mixed, composite microstructure with high strength but also good ductility and toughness [37].

2.3.3 Mechanical Properties

The work of Cola [4] provides various types of experimental data for mechanical properties of flash processed steels. His work focused on AISI 4130 and AISI 4140 steels. The comparison amongst flash processed AISI 4130, AISI 4140 and other high strength low alloy (HSLA) steels has been made. The result showed a promising outcome for flash processed steels as they overcome typical HSLA steels in the aspects of strength, ductility and armor piercing tolerance. The results can be illustrated below.

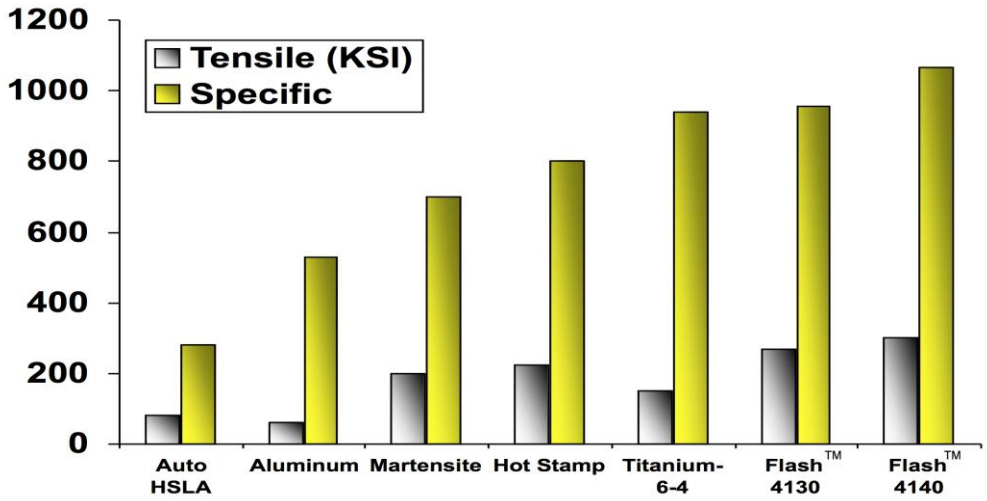

Figure 24. Tensile strength of flash steels compared to other HSLA steels [31]

It is clear that flash processed steels possess better strength compared to other HSLA steels, even for the martensite ones. Also, the specific strength for flash processed steels is better and would reduce the cost of manufacturing materials [4, 37].

Figure 24 also points out that flash processed steels have high ductility, since the percent elongation values are outstandingly high, compared to other high strength material [4, 37].

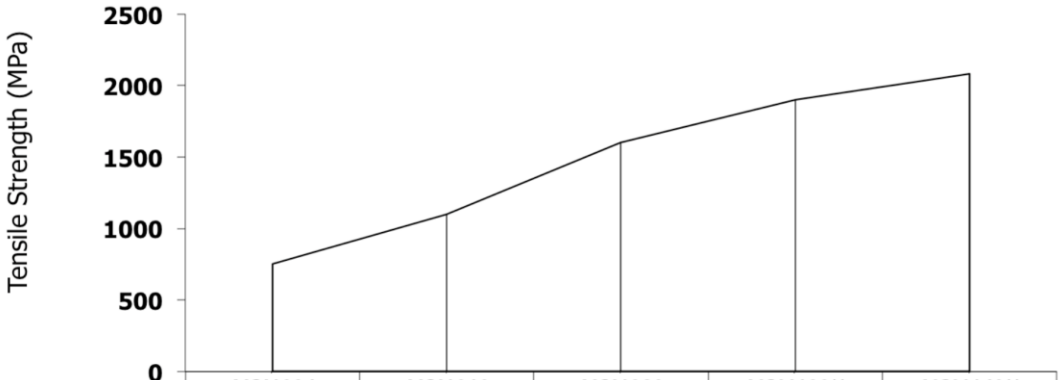

	AISI1004	AISI1010	AISI1020	AISI4130**	AISI4140**
Tensile (MPa)	750	1100	1600	1900	2080
Elongation A50	8.60%	8.50%	9.50%	11.00%	10.00%
%wt Carbon	0.036	0.104	0.211	0.305	0.402
%wt Iron	99.5	99.4	98.4	97.6	97.2

Figure 25. Ductility of flash processed steels presented together with their tensile strength **[**37**]**

All the results pointed out that flash bainite steels show promising characteristics as a future materials in steel industry and that, the flash process should be considered as one of the innovative heat treatment process since it saves both process time and material costs. However, the work can still be improved, since Cola's work focused mainly on certain types and combinations of steels. The more detail explanation on morphology and microstructure aspect could be made for more understanding of how to develop this type of microstructure and mechanical properties. Also, the refined process of flash bainite still can be developed in the future so that it provides various options of heat treatment for other kinds of steel. These are the main purposes of this study.

3.0 EXPERIMENTAL PROCEDURES

3.1 HEAT TREATMENT CYCLE

To understand the behavior and formation of flash processed bainite, similar process of heat treatment to typical flash process has to be considered. The proposed cycle in this study has 2 heating and cooling rates; slow (40 °C/s heating and 100 °C/s cooling) and fast (80 °C/s heating and 200 °C/s cooling). Heat treatment has been done to each of the specimens individually and the heat-affected zone for each one is in the central region (around 20 mm in diameter). Therefore, the study of the heat-treated steels in this research focused mainly on the central part of the steels (Figure 26).

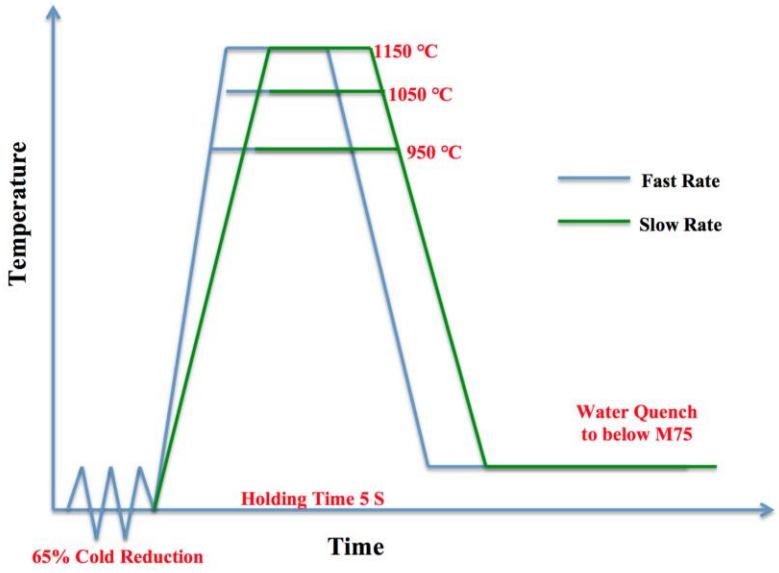

Figure 26. Heat treatment diagram of this research

3.2 MATERIALS CONDITIONS

Materials used in this research are high strength low carbon alloy. The carbon content in each of the specimen is 0.1 percent with additional alloying elements. The specimens can be classified into 2 groups: 2A and 2B. The first group, 2A, is the steel without vanadium (V) addition. They have been preheated with 525 °C coiling temperature and cold rolled with 65 percent cold reduction. The second group, 2B, has same initial condition but with vanadium addition of 0.06 percent. The composition of the steels both 2A and 2B are shown in Table 2.

Table 2. Chemical composition for 2A and 2B steels

Composition	**Content, weight percent**	
	2A	**2B**
C	0.1	0.1
Mn	1.75	1.75
P	0.01	0.01
S	0.002	0.002
Si	0.4	0.4
Cr	0.5	0.5
Mo	0.3	0.3
V	-	**0.06**
Al	0.03	0.03
N	0.006	0.006

Note: 525 Degree C coiling Temperature, 65% Cold Reduction

The terminal temperatures of the heating cycle were determined by studying the A_{r3} temperature of the steels. For the steels 2A and 2B, the A_{c3} temperature has been simulated using JMatpro software version 7.0. The results are shown below (Figure 27).

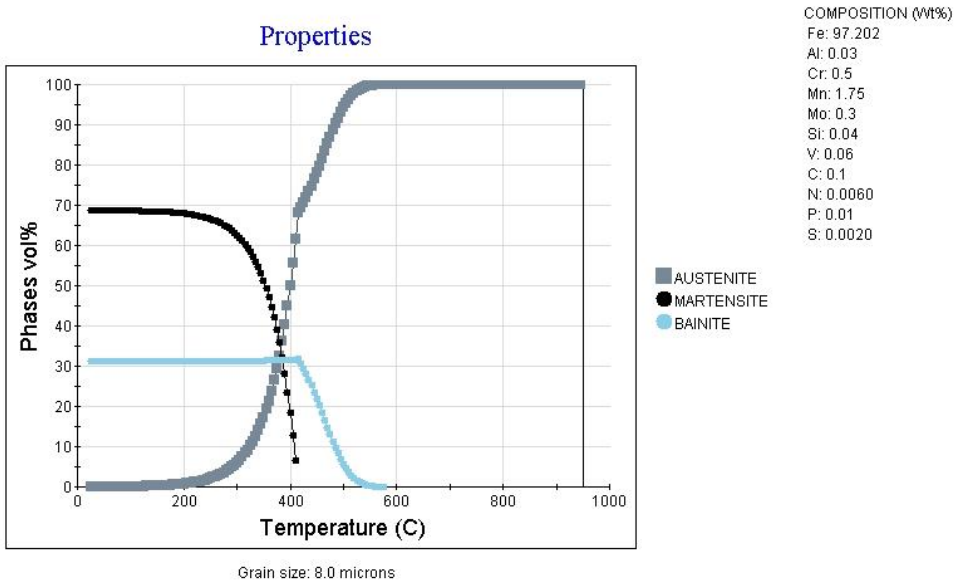

Figure 27. Ac3 temperature for 2A and 2B steels, ~820 °C

With the A_{r3} temperature of 820 °C, the terminal temperature of 950, 1050 and 1150 °C were chosen. The higher temperatures were to confirm the assumption that carbides dissolution plays an important role in developing the bainite in the final microstructure. At 1050 and 1150 °C, carbides should dissolve almost completely and hence will result in other type of microstructure in the final rather than flash bainite.

The specimens in this study were heat treated with the same heat treatment cycles. The dimensions of the specimen are 50mm x 10mm x 1.26mm thickness before and after heat treatment. The data of both specimen conditions and heat treatment parameters can be summarized as in Table 3.

Table 3. Heat Treatment Plan for Flash Bainite

Steel	**2A & 2B (Both steels get the same heat treatment)**		
	Reheat Temperature, °C		
	950	1050	1150
Holding Time	5 s	5 s	5 s
Heating and Cooling Rate (Fast)	+80 °C/s, -200 °C/s **(950_2AF and 950_2BF)**	+80 °C/s, -200 °C/s **(1050_2AF and 1050_2BF)**	+80 °C/s, -200 °C/s **(1150_2AF and 1150_2BF)**
Heating and Cooling Rates (Slow)	+40 °C/s, -100 °C/s **(950_2AS and 950_2BS)**	+40 °C/s, -100 °C/s **(1050_2AS and 1050_2BS)**	+40 C/s, -100 C/s **(1150_2AS and 1150_2BS)**

Note: Total 6 pieces for each steel, 50mm x 10mm x 1.26mm thickness

After heat treatment, the steels were morphologically studied and analyzed. The microstructure were studied and discussed in terms of its formation, both of which require the certain steps of work and methodology.

Figure 28. 2A group of specimens after heat treatment

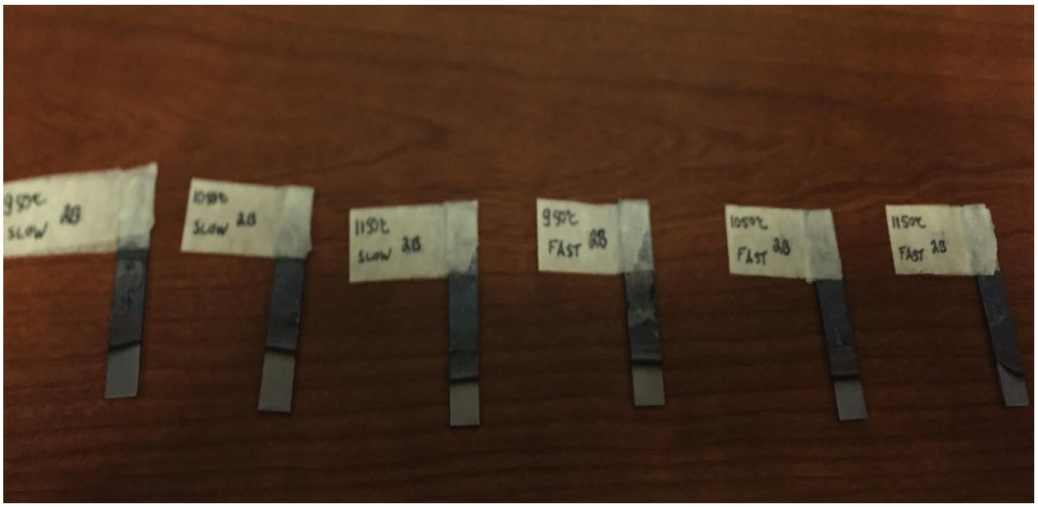

Figure 29. 2B group of specimens after heat treatment

3.3 SURFACE PREPARATION

After heat treatment, each strip of steel was cut down on both end and only the central region of about 20 mm diameter was further studied. The central region, as mentioned before, is the area where the heat during the process uniformly affected the microstructure of the steels. The cut-down samples were mounted and surface-cleaned before further experimentation. The procedures of surface preparation are described below.

3.3.1 For Optical Microscopic Study

Before the optical microscopic study, the samples were ground on the surface with silicon carbide paper with 400, 600, 800 and 1,200 grits, respectively. After the grinding, the samples were polished in 0.05 microns alumina polishing solution for 1 hour. The surface then, would be cleaned with water, rubbed thoroughly with cotton and dried.

3.3.2 For Scanning Electron Microscopic Study

The similar process of surface preparation for the optical microscope study had been done. The surface of the samples was ground again to reveal the fresh and clean surface, this time only from 800 to 1,200 grits. The samples were polished again for 1 hour in the same solution and cleaned in the similar way.

3.3.1 For Electron Backscatter Diffraction Study

The surface preparation for Electron Backscatter Diffraction (EBSD) study must be done carefully, since the magnification of EBSD is significantly higher than OM or SEM. After grinding, the samples were polished in the same solution for at least 3 hours each. This is to increase the surface texture and ensure the cleanliness of it.

3.4 MICROSTRUCTURAL ANALYSIS

The procedures of data collection and microstructural analysis are discussed in the following paragraphs. Three different techniques and devices have been utilized in this research, which are the Optical Microscope, the Scanning Electron Micrograph and the Electron Backscatter Diffraction.

3.3.1 Optical Microscopy (OM)

Samples after surface finish were studied through optical microscope using Nital-etching technique. Nital is a mixture of nitric acid and alcohol commonly used for etching steels. It is especially suitable for revealing the microstructure of carbon steels. In this study, 2% concentration of nital acid was used. The nital-etching revealed the martensitic-microstructure of the samples and categorized samples into 2 groups: 4 samples with a chance of having bainite and 8 samples without. The results of the nital-etched samples can be found in the following section.

Figure 30. Optical Microscope used in this research

After the Nital etching, the samples were re-grinded and re-polished. The surface of the samples were cleaned and prepared for Picral etching.

Picral Etch is a common etchant for etching heat-treated steels. It contains 4% picric acid in denatured ethanol alcohol. This etchant is listed in ASTM standard E 407 as No. 76 Picral. The picral etch revealed the pre-austenite grain size and boundary. This was to confirm the trace of carbon concentration gradient along the grain boundaries, which in the end will transform into bainite in the final microstructures. Also, it revealed the small trace of martensite inside the grain, which can further confirm that the flash bainite microstructures that have been developed in these samples, formed in the same way as the typical flash process does.

Another technique that has been used in this research was LePera etching. LePera etching is anodic surface layer etching technique using 50 ml $Na_2S_2O_5$ 1% in aqueous dilution, 50 ml

picric acid 4% in ethanol to etch the samples surface. The samples were etched in the etchant for 20 seconds for each solution. The results showed the different colors for each phase or microstructure in steels. Ferrite appears to be blue, bainite appears to be brown and martensite appears to be white. Carbon and silicon contents in steels usually have a strong influence on the ferrite color. With more carbon, ferrite appears to be darker [38]. By using this technique, each phase can be distinguished in the optical microscope.

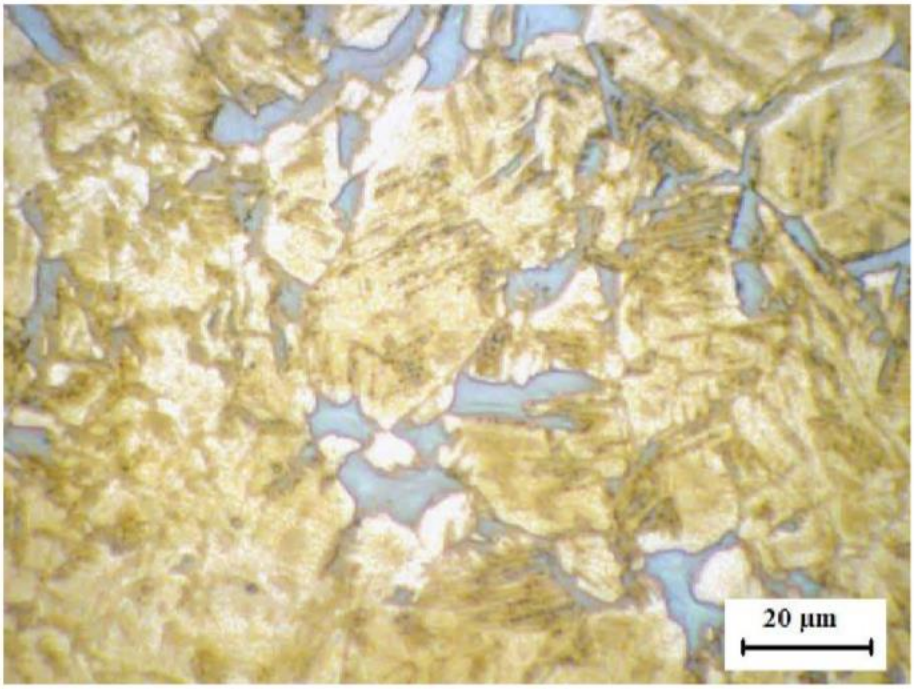

Figure 31. LePera etch result of low alloy carbon steel [38]

3.3.2 Scanning Electron Microscopy (SEM)

Scanning electron microscopy played an important role in this research. The samples with traces of bainite along grain boundaries shown on OM were scanned and studied thoroughly using the SEM. With the high magnification and resolution scan, the closer looks to the surfaces of the samples were done. The microstructures of the samples were studied and compared

amongst each group. Four samples with flash bainite have been scanned for further confirm on the characteristics of bainite and martensite in the microstructures. Eight samples without flash bainite have been scanned to further confirm that there was no bainite in the microstructure, only martensite. The magnifications that have been used were 2000, 5000 and 8000 times with 10 kV electron beam and 3 spots value.

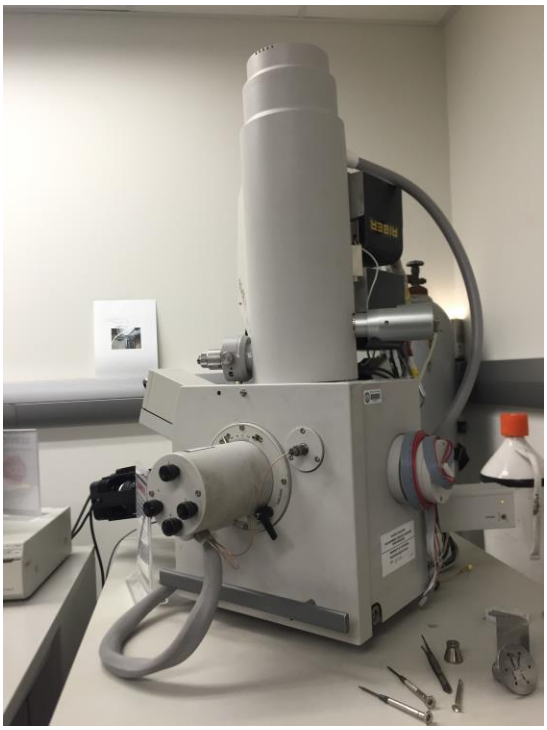

Figure 32. The microscope for SEM and EBSD

SEM returned the images of microstructures, in which different phases can be distinguished. The brightness of each phase are different in the SEM image, and also, the essential appearances are different just like in the OM. Martensite appeared to be needle-like and mainly existed inside the grain boundary. Bainite appeared to be plate-like, in this case, and existed both along grain boundaries and inside the grains. More discussion will be made in the following section.

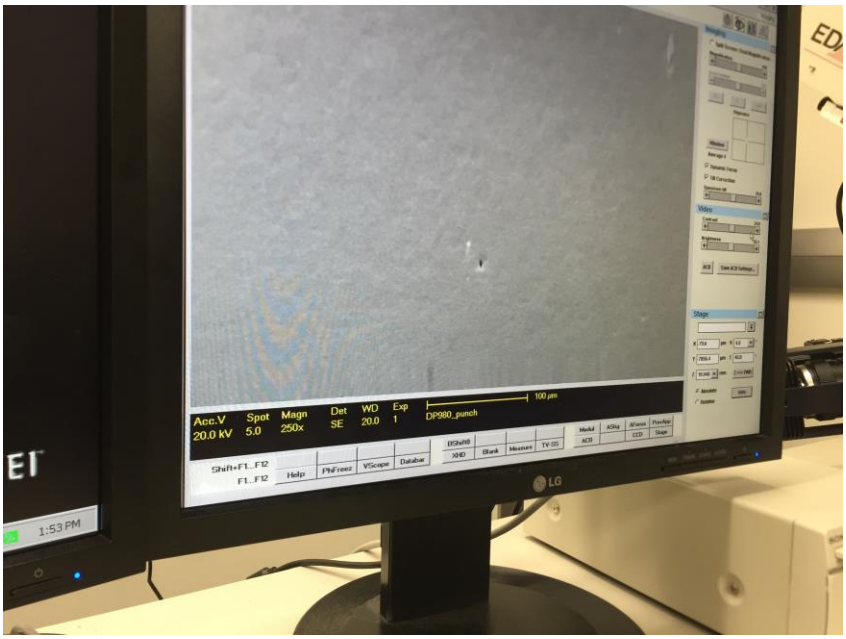

Figure 33. Human interface of SEM control software

3.4.1 Electron Backscatter Diffraction

For 4 samples with flash bainite, more detailed experiments were accomplished using Electron Backscatter Diffraction (EBSD) technique. EBSD indicated more information in crystallographic terms. The setup of the EBSD was 20 kV electron beam with 5 spots value. The estimated grain size of the sample was less than 5 microns with the scanning rate of the EBSD was 60 x 60 microns and 0.2 micron step size. The results of each sample were compared amongst each other for more information on morphology and the characteristics. EBSD provided the information of misorientation angle, grain boundary angle and inverse pole figure map.

These types of information were crucial in analyzing and differentiating martensite from bainite. Also, it helped in differentiating between flash bainite samples and developed more understanding of the factors of heat treatment, which have an impact on final characteristics of steels.

Figure 34. The setup of the microscope and beam gun for the EBSD

The values of Kernel Average Misorientation (KAM) have been used in the discussion section. The KAM function is used to determine local values of intragranular lattice rotation. KAM is numerically defined as the average of misorientation between the pixel of interest and the entire specified nearest neighbor pixels. The KAM is then defined as the average misorientation between the pixel at the center of the kernel, and all points at the perimeter of the kernel are measured. For a given point, the average misorientation of that point with all of its neighbors is calculated with the provision that misorientations exceeding some tolerance value (maximum misorientation, 5°) are excluded from the averaging calculation [39].

3.5 HARDNESS TEST

Hardness was chosen as a representative of mechanical properties of the materials. Each of the samples has been tested with Vickers Hardness testing procedure. The tests were conducted using a load 300 gf. 30 indents have been put on each sample across the length in the central region. The average hardness values for each sample have been calculated in the unit of HV.

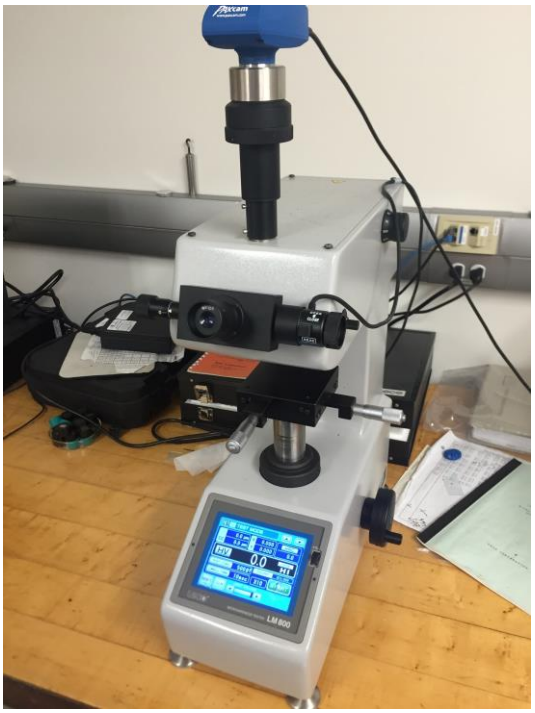

Figure 35. Vickers Hardness Testing Machine

4.0 RESULTS AND DISCUSSION

Sets of experiments have been done in this research to study the characteristics and confirm the final microstructures of the samples. The results will be presented and discussed in the following section.

4.1 OPTICAL MICROGRAPHS

Twelve samples were studied with OM from 10 to 100 magnifications. For the study after nital etching, the results showed that 4 of the samples that were heat-treated to 950 °C revealed some different microstructures, which consist mainly of martensite microstructures (Figures. 36 – 40).

4.1.1 Nital-etched Samples

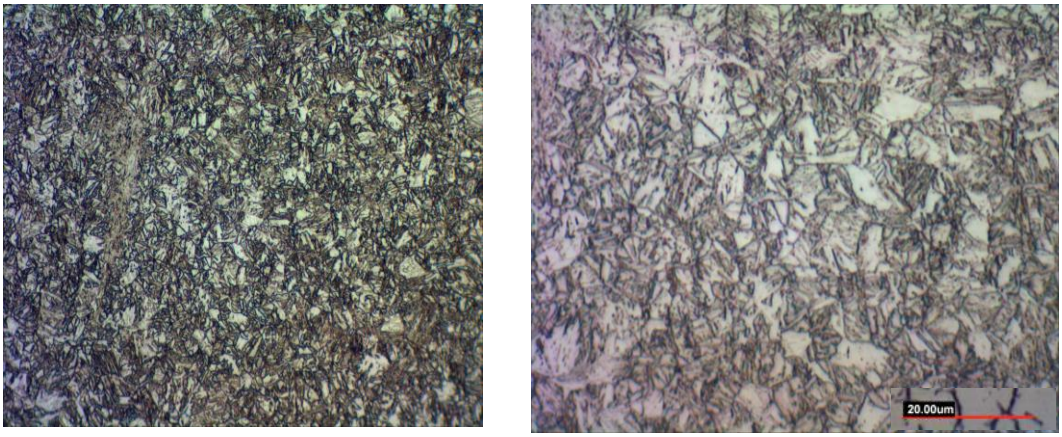

Figure 36. Optical micrographs of 2B steel, heat-treated to 950 °C with a fast rate (950_2BF) at 40x and 100x (Left to right)

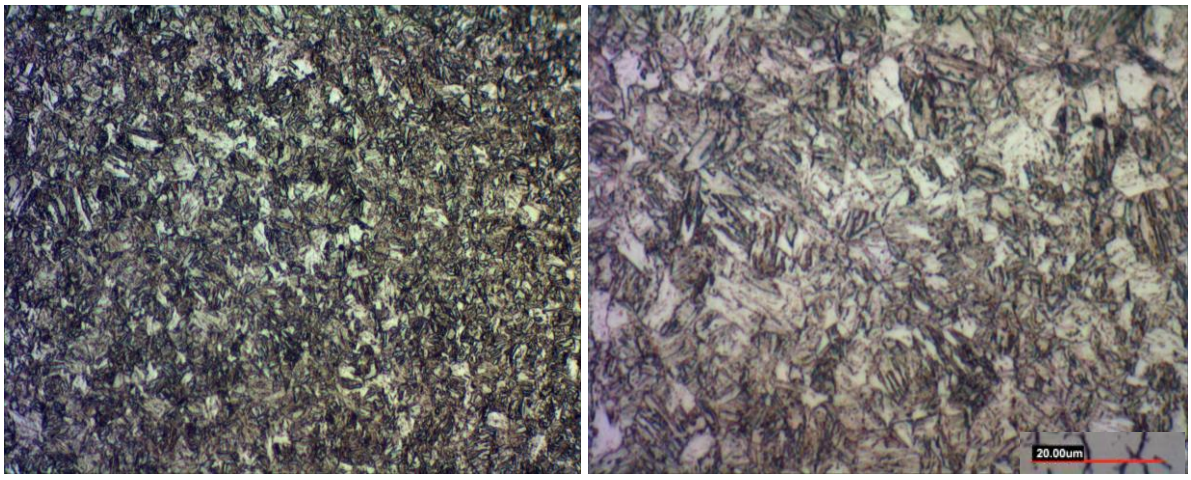

Figure 37. Optical micrographs of 2A steel, heat-treated to 950 °C with a slow rate (950_2AS) at 40x and 100x (Left to right)

From Figure 36 and Figure 37, the microstructures revealed the majority of martensite and some part of plain white microstructures. The plain white microstructures were assumed to different microstructures apart from martensite. Moreover, it should be noted that the fraction of white microstructures in the fast rate samples are higher than the slow ones. Presumably, this microstructure is a bainite, which means the samples were the flash bainite, the higher fraction of bainite was due to the dissolution of carbides during the heating phase. Slow heating and cooling rate means longer time for austenite to nucleate and dissolve carbides, hence reducing carbon concentration gradients, resulting in less bainite fraction in the end [3, 4]. However, further confirmation for the type of microstructure still had to be made with other experimental techniques, SEM and EBSD.

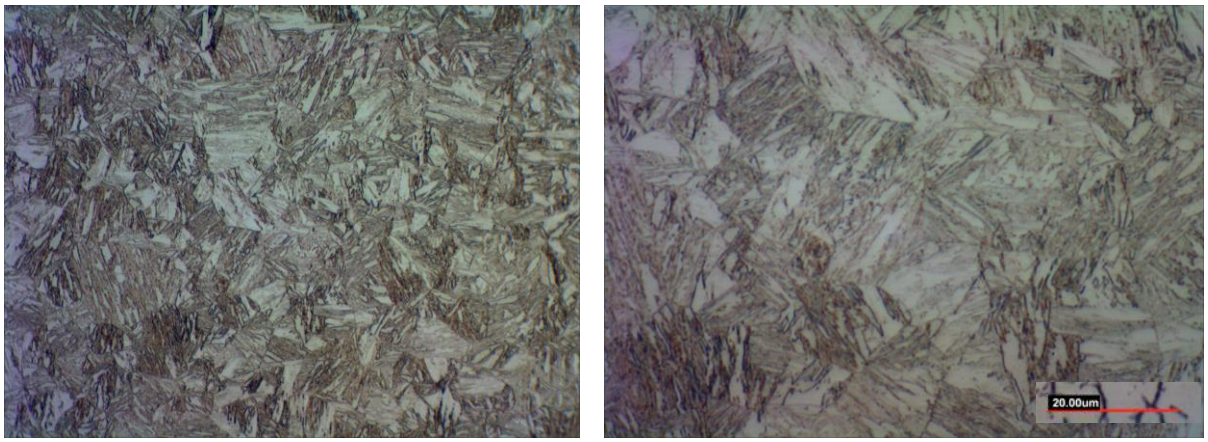

Figure 38. Optical micrographs of 2B steel, heat-treated to 1050 °C with a slow rate (1050_2BS) at 40x and 100x (Left to right)

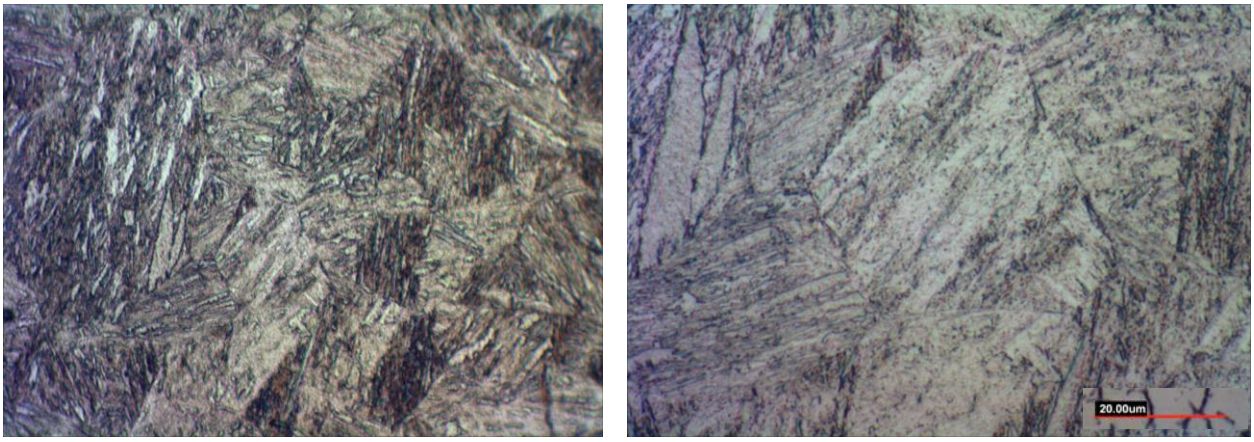

Figure 39. Optical micrographs of 2A steel, heat-treated to 1150 °C with a fast rate (1150_2AF) at 40x and 100x (Left to right)

In Figure 38 and Figure 39, the microstructures showed nearly 100 percent martensite. The needle-like characteristics of the microstructures can be seen across the samples. The martensite microstructure is due to the heating period is longer than the samples heat-treated at 950 °C so, it allows carbides to dissolve in greater extent.

This group of samples, both 2A and 2B, heat-treated at 1050 and 1150 °C were classified as the samples with no flash bainite. However, some of the plain white fraction can still be found in both samples with heat treatment of 1050 and 1150 °C. This microstructure was further studied with SEM and EBSD in the next step. The comparison between samples with and without bainite has been made in figure 40. The difference in the microstructure can be clearly observed. The sample on the left (950_2BF) shows several plain white fraction in the boundaries, meanwhile the sample on the right (1050_2BS) resembles martensite morphological appearance and show significantly less amount of plain white phase.

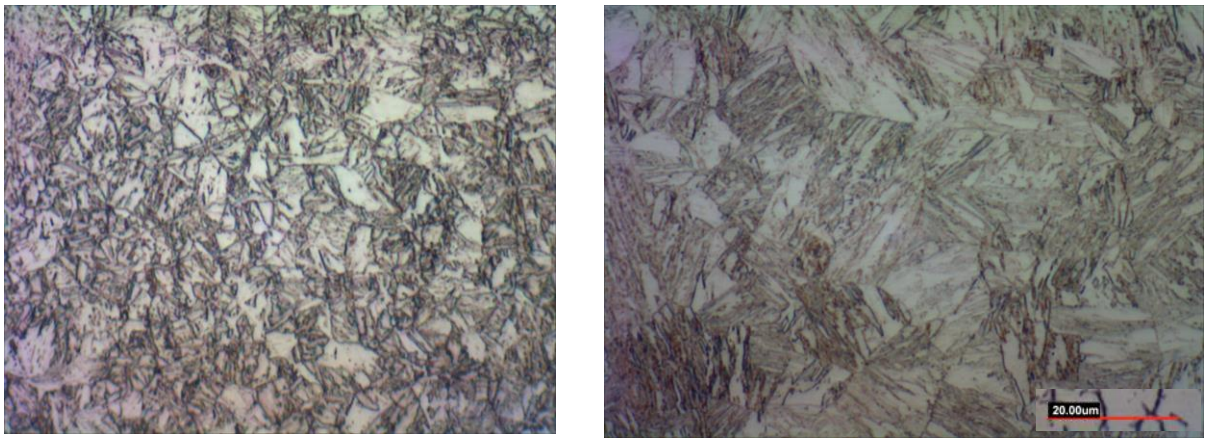

Figure 40. Comparison between 950_2BF and 1050_2BS samples at 100x (Left to right)

4.1.2 Picral-etched Samples

Picric acid has been used to reveal the pre-austenite grain size of the samples from the heat treatment. The grain size indicated the effects of composition, treatment temperature and heating/cooling rate on the microstructures. Typically, higher temperature heat treatment should result in coarser grain size, also the same for slower heating rate [40, 41]. Also, 2B samples consist of 0.06 percent of vanadium; this should result in finer grain size after the heat treatment, since vanadium has an effect of pre-austenite grain size refining [1, 41]. The results of the picral-etched samples are shown below (Figures. 41 – 44).

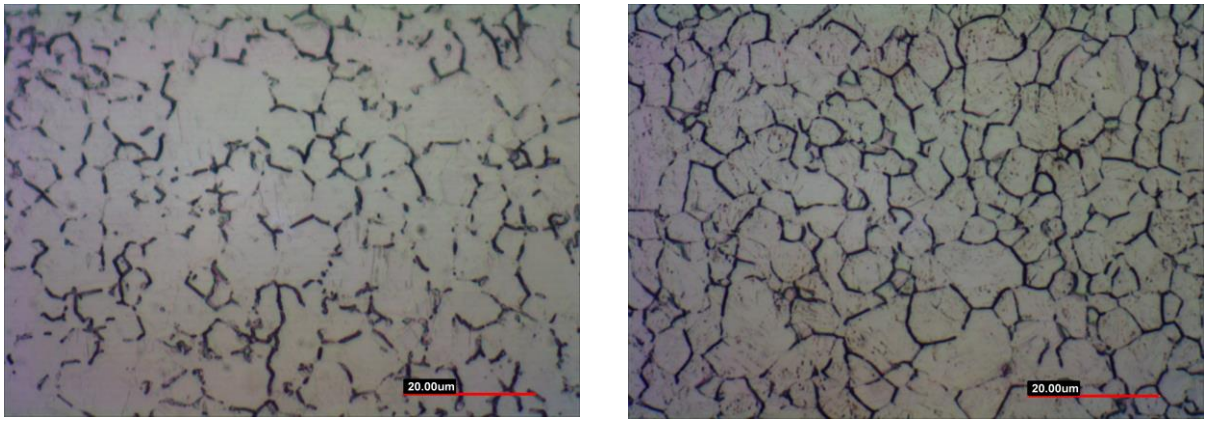

Figure 41. Picral-etched micrographs of 2A samples, heat-treated at 950 °C slow and fast rate (Left to right), 100x magnification

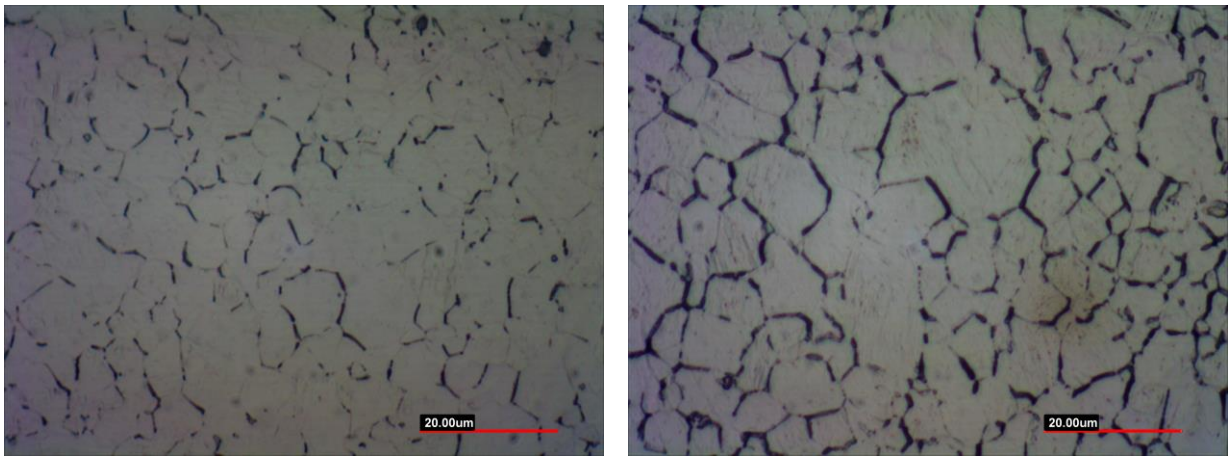

Figure 42. Picral-etched micrographs of 2B samples, heat-treated at 950 °C slow and fast rate (Left to right), 100x magnification

Comparison between the micrographs of the samples with slow and fast rate are shown in Figure 41 and Figure 42, for both 2A and 2B samples, heat-treated at 950 °C. From the Figures, it can be concluded that the higher heating rate resulted in finer grain size in the final microstructure, conforming previous researches. Also, it should be noted here that the grain boundaries in both samples 2A and 2B, which were heat-treated at 950 °C, are thick and clear.

This is the case no matter what the heating rates are. The assumption has been made that clear grain boundary was the trace of carbon along the grain boundary. These carbon gradients along the boundaries were the origin of plate-like bainite along the grain boundaries in the final microstructures. This result was further confirmed with SEM results.

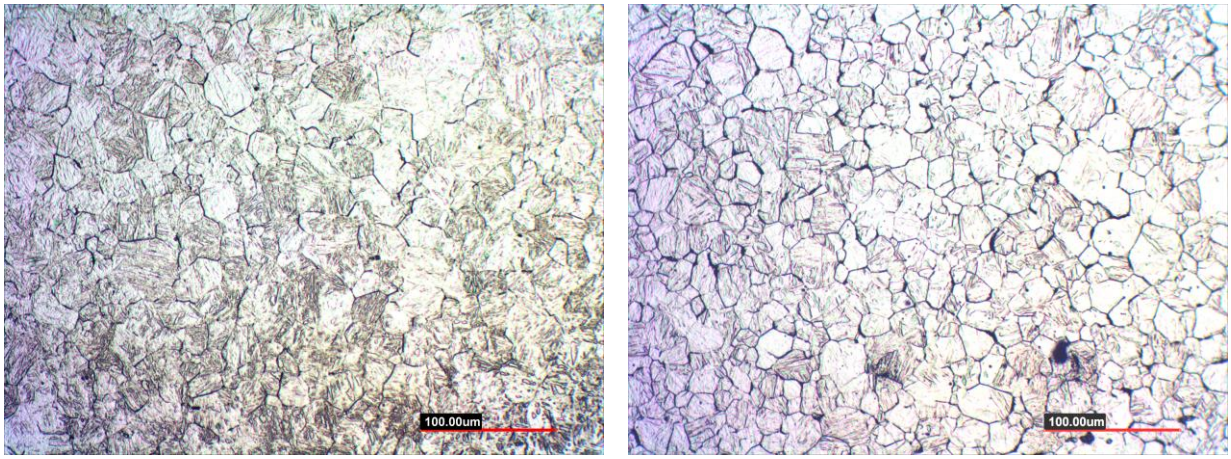

Figure 43. Picral-etched micrographs of 2A and 2B samples, heat-treated at 1050 °C slow rate (Left to right), 20x magnification

Figure 43 illustrates the effect of vanadium on the grain size of the final microstructures. As the results show, 2B sample with the vanadium addition has finer grain size than 2A sample when other factors are identical. Vanadium suppresses the grain growth during recrystallization, hence leading to finer grain size after the heat treatment. The finer grain size results in higher strength and hardness of the final properties, theoretically. Also, it should be noted the difference for the outline of grain boundaries in both samples, compared to 950 °C heat-treated samples. The outline of the grain boundary are less strong for higher temperature heat-treated samples,

presumably that, this was due to the lack of carbon gradient along grain boundaries since most parts of the carbides had already dissolved.

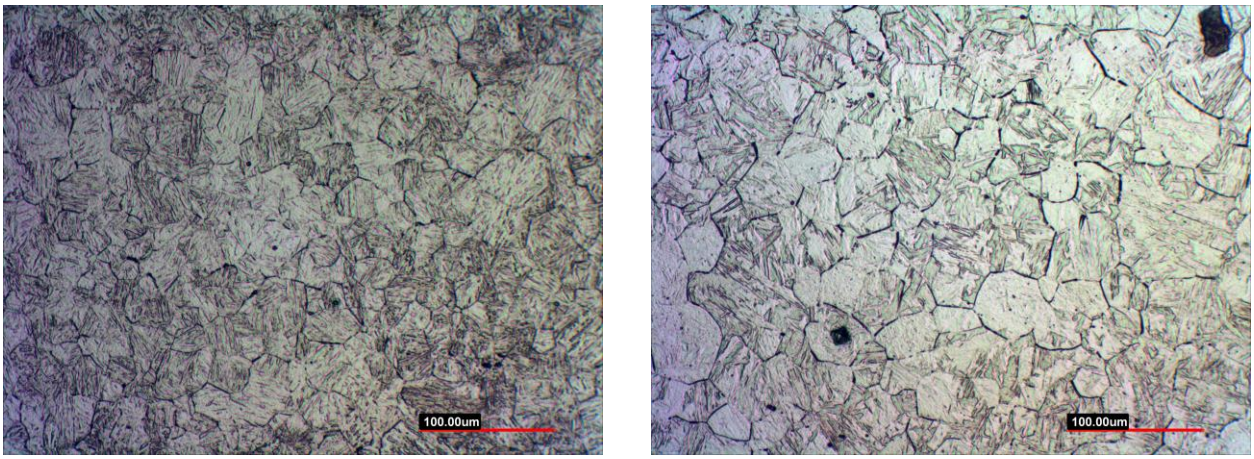

Figure 44. Picral-etched micrographs of 2B samples, heat-treated at 1050 and 1150 °C fast rate (Left to right), 20x magnification

Figure 44 depicted the effect of heat treatment temperature on the final grain size. It can be clearly seen that with higher heat treatment temperature, grain size becomes bigger. This was because at high temperature, the nucleation rate of ferrite is low and led to coarser grain size when the process is finished. The weak outline of grain boundaries can also be observed here, since the samples were heat-treated at 1050 and 1150 °C, stressed again that, at even higher temperature than A_{r3} temperature, carbides dissolved almost completely.

Moreover, the grain size of each sample measured using ImageJ software can be summarized in Table 4, below.

Table 4. Grain size measurement of 12 samples

Steels	Heat Treatment	Grain Size (microns)	Standard Deviation
2A	950 °C, Slow Rate	6.6	5.4
	950 °C, fast rate	6.2	5.2
	1050 °C, slow rate	26.5	22.1
	1050 °C, fast rate	21.5	18.5
	1150 °C, slow rate	35.7	29
	1150 °C, fast rate	29.6	25.3
2B	950 °C, Slow Rate	6.3	5.3
	950 °C, fast rate	4.8	4.1
	1050 °C, slow rate	20.0	15.1
	1050 °C, fast rate	19.2	15.8
	1150 °C, slow rate	35.6	27
	1150 °C, fast rate	24.9	19.1

However, OM results did not show details morphology of the microstructure, so other techniques needed to be used. SEM and EBSD play an important role in microstructure and crystallography study, and were utilized in this research.

4.1.3 LePera-Etched Samples

The samples have been etched with LePera etchant to study and differentiate between different phases in the microstructure, to confirm the structures developed in the final results of each one. The results are shown in Figures 45-47.

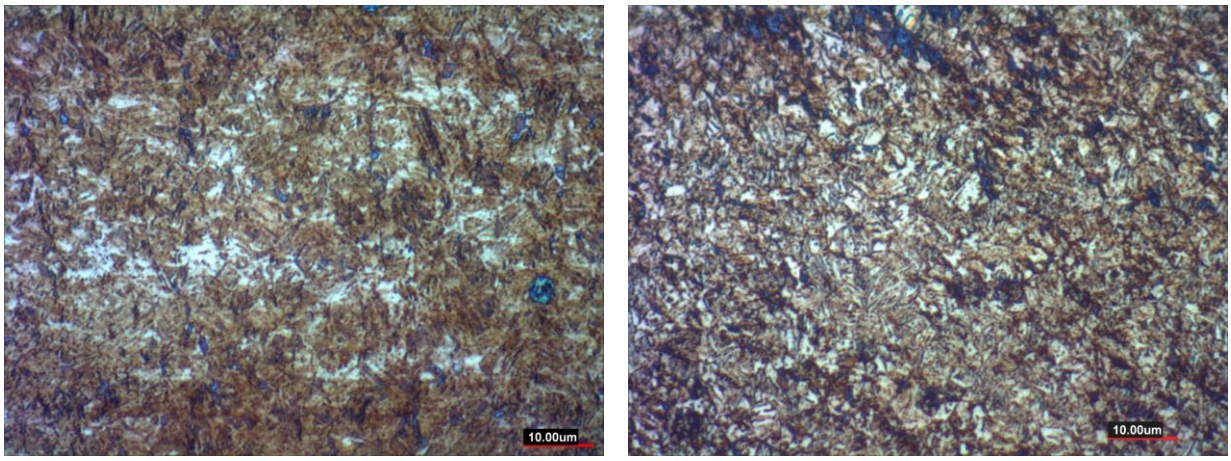

Figure 45. LePera-etched results of 950_2AF and 950_2AS samples at 100x (Left to right)

Figure 45 shows result of LePera etching of 950_2AF and 950_2AS samples. The differences in the color of each phase can be detected but not clearly distinguished. The dark blue regions in the photos represent ferrite phase in the microstructure, while the white and light-brown regions represent martensite and dark brown regions represent bainite phase. Martensite phase can be found dispersedly and clearly in the microstructure since it is the brightest color. Bainite can also be spotted but not clearly stands out amongst other phases, but the fraction of bainite is still noticeable. However, fraction ratios for each phase cannot be easily measured since some of the phase co-exist and cannot be clearly classified.

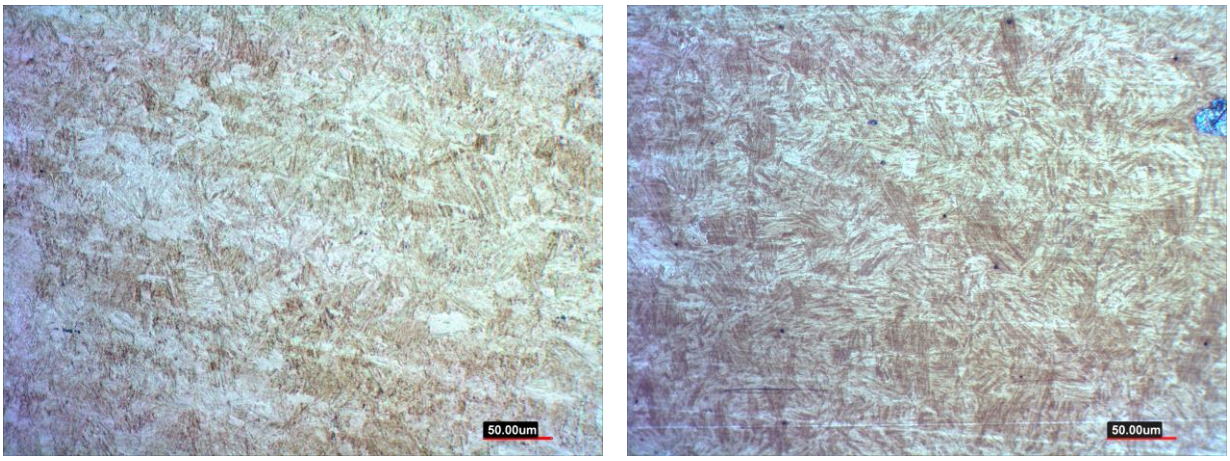

Figure 46. LePera-etched results of 1050_2BS and 1150_2AF samples at 20x (Left to right)

Figure 46 shows LePera etching results of 1050_2BS and 1150_2AF samples. It is can be clearly seen that the microstructure in these 2 samples are needle-like, which resemble martensite microstructure. Also, the microstructure shown in this figure is all white and light brown colors. Hence, it can be assumed that in high temperature heat-treated samples, the final microstructure is almost 100% martensite. The comparison between low temperature and high temperature heat-treated results can be found in Figure 47.

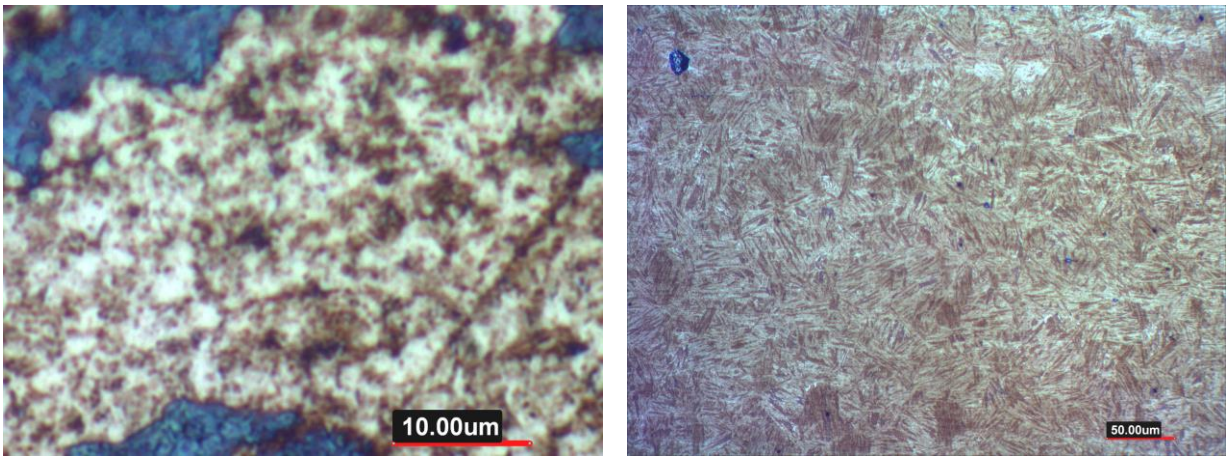

Figure 47. Difference between low temperature (950_2BS) and high temperature (1150_2AF) heat-treated results (Left to right)

4.2 SCANNING ELECTRON MICROGRAPH

After the observation from OM, the samples with the trace of bainite in the microstructures were further examined with SEM. With SEM, the plain-white microstructures from OM results can be confirmed for their type. Four samples (950_2AS, 950_2AF, 950_2BS and 950_2BF) have been thoroughly studied using SEM, moreover, the rest of the 8 samples were also studied to confirm that there were no significant amount of bainite in the final microstructure, and that, the formation of flash bainite developed in this research conformed to the typical type. The results are shown below.

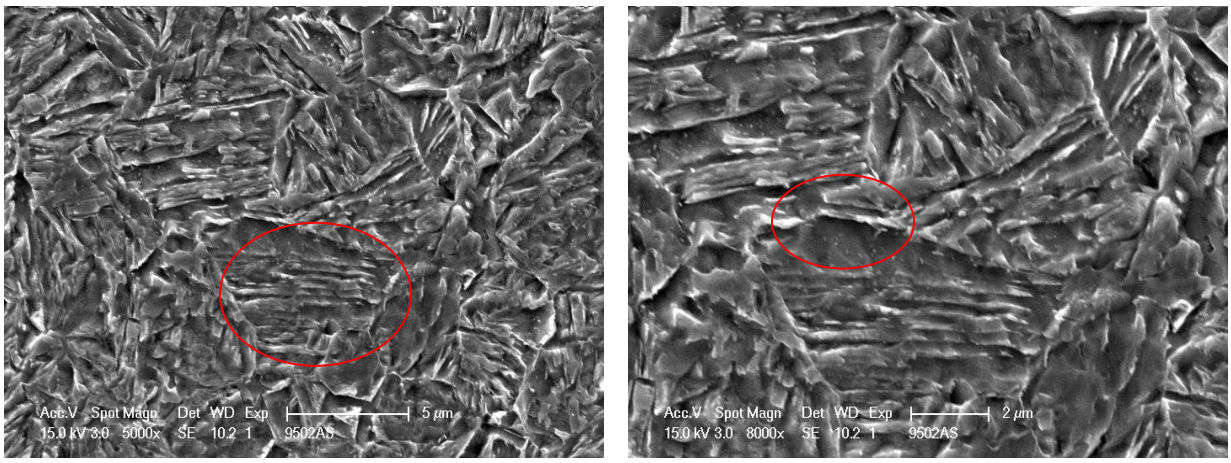

Figure 48. SEM results of 2A sample, heat-treated at 950 °C with slow rate (or 950_2AS), under 5000x and 8000x magnification (Left to right)

Figure 48 shows the results of the SEM for 950_2AS sample. The red circle on the left shows the plate-like bainite microstructure within the grain. The metallographic appearance of this structure resembles the appearance of upper bainite (more specifically: bainitic ferrite), which is a plate-aggregated sheave. The nucleation site of the bainite can be assumed to be on the edge of the grain. The red circle on the right further confirms the formation of bainite along grain boundaries with the bainite microstructure along the outline. This conforms to the explanation of how bainite forms from the low carbon gradient along the grain boundaries, which has been explained in [3] and [4].

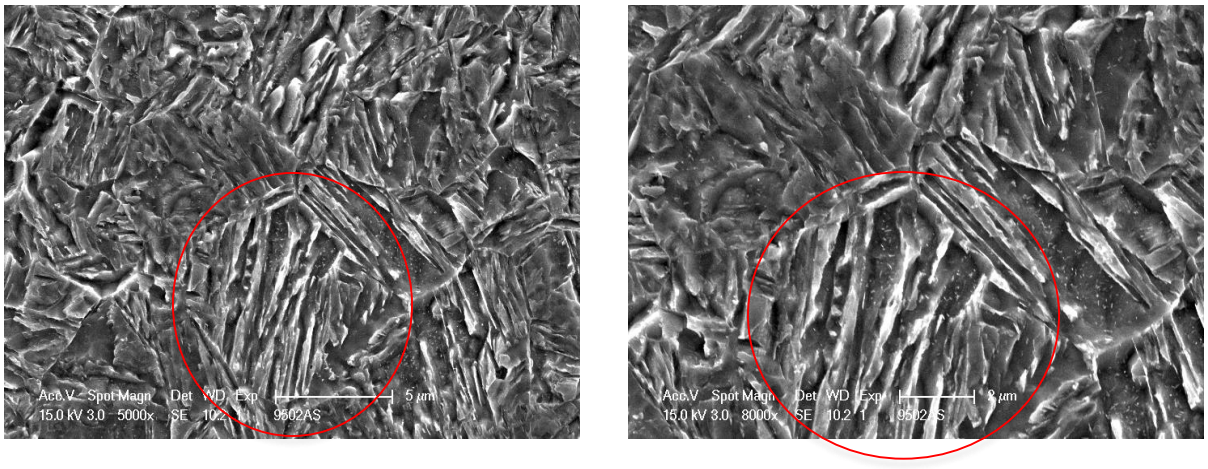

Figure 49. Another SEM results of 950_2AS sample, under 5000x and 8000x magnification (Left to right)

Figure 49 shows another result for sample 950_2AS, from another region on the surface. The red circles in both figures show the martensite microstructure in the grain. The needle-like shape martensite within the grain can be found dispersed in the microstructure. This characteristic resembles the appearance of lath martensite or low carbon martensite, which in this case, has carbon concentration of around 0.1 percent. Martensite forms from the high carbon gradient regions within austenite grains during the quenching. The high carbon gradient regions

in austenite grains are the regions with partially dissolved carbides, normally within the inner part of the grains.

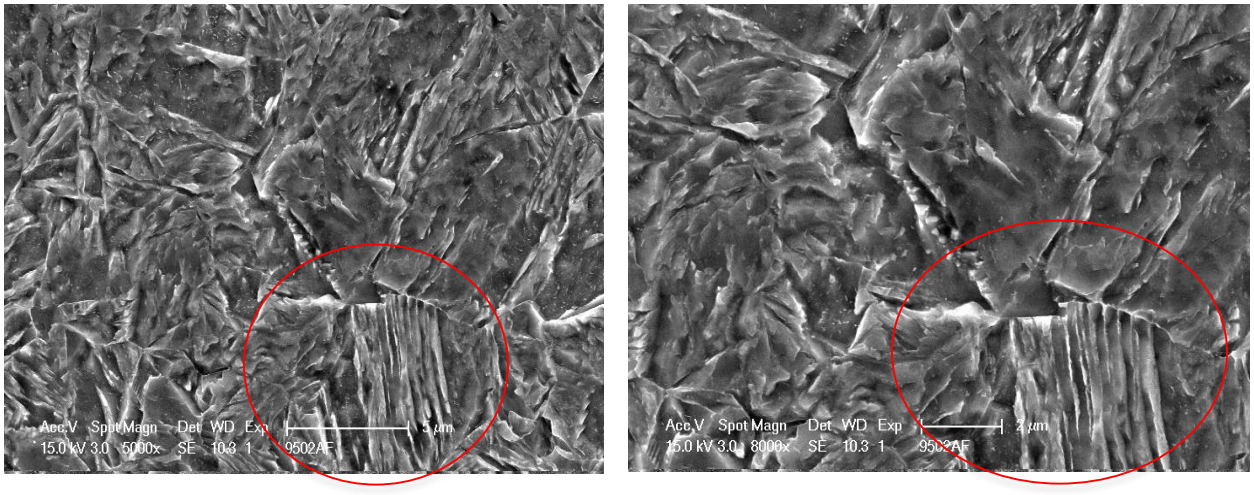

Figure 50. SEM results of 2A sample, heat-treated at 950 °C with fast rate (or 950_2AF), under 5000x and 8000x magnification (Left to right)

Figure 50 shows results for sample 950_2AF in a similar manner. The microstructure in the red circles shows the characteristics of bainite, identical to the one in 950_2AS. The sheave of bainite plates extends from the grain boundary to the center. Also, some trace of the bainite microstructure along the outline of the boundary shows. This result further confirms the formation type of bainite in the flash-processed steel.

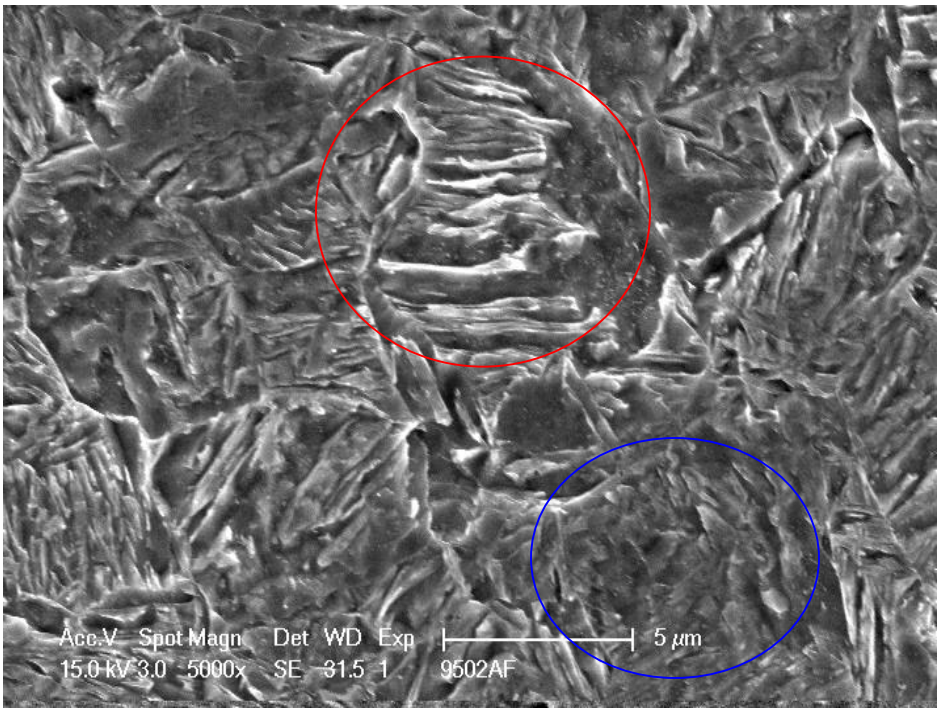

Figure 51. Another SEM results of sample 950_2AF, showing bainite microstructure along with martensite microstructure (red and blue circle, respectively) at 5000x magnification

Figure 51 shows another result for sample 950_2AF. The bainite microstructure in the red circle along with martensite microstructure in the blue circle, have the characteristics similar to those in sample 950_2AS.

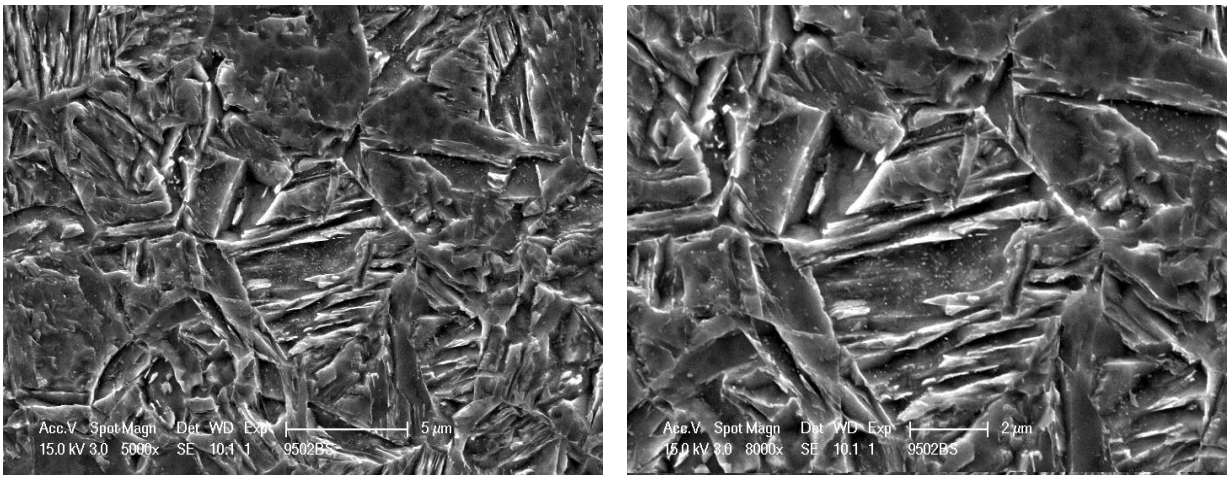

Figure 52. SEM results of sample 2B, heat-treated at 950 °C with slow rate (or 950_2BS), under 5000x and 8000x magnification (Left to right)

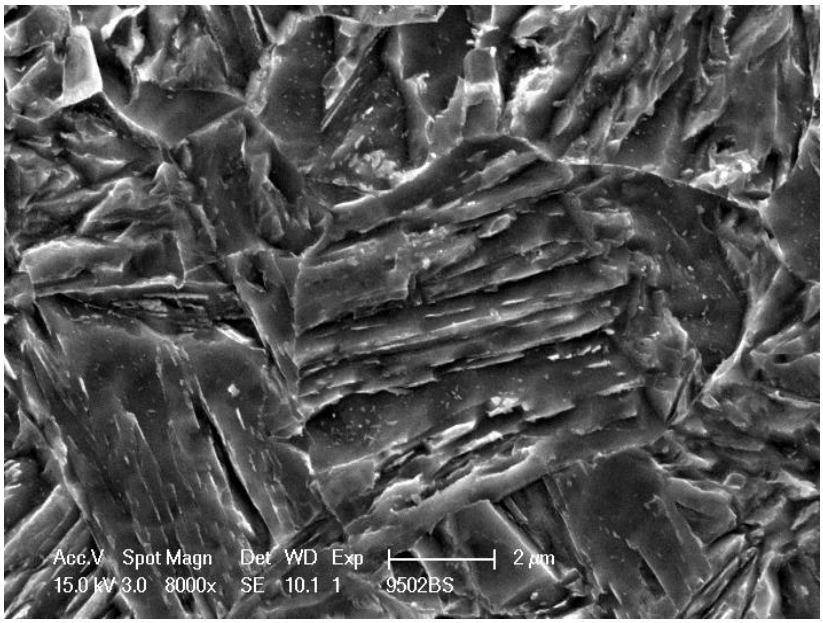

Figure 53. Another SEM results of sample 950_2BS, showing bainite microstructure in the central grain of the micrograph under 8000x magnification

The results of sample 950_2BS are shown in Figure 52 and Figure 53. In Figure 52, bainite grain in the center co-exists with martensite microstructure disperses around the region. The austenite grain in the center shows strings of cementite, which is a clear sign of bainite formation. Meanwhile, in Figure 53, bainite central grain shows the characteristic of plate-like appearance.

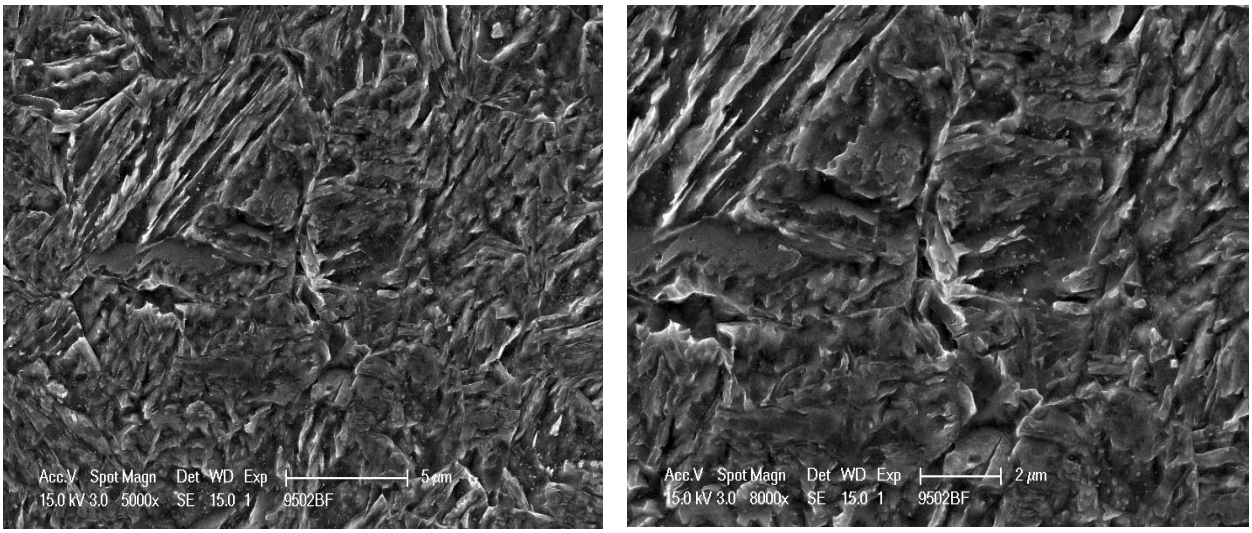

Figure 54. SEM results of sample 2B, heat-treated at 950 °C with fast rate (or 950_2BF), under 5000x and 8000x magnification (Left to right)

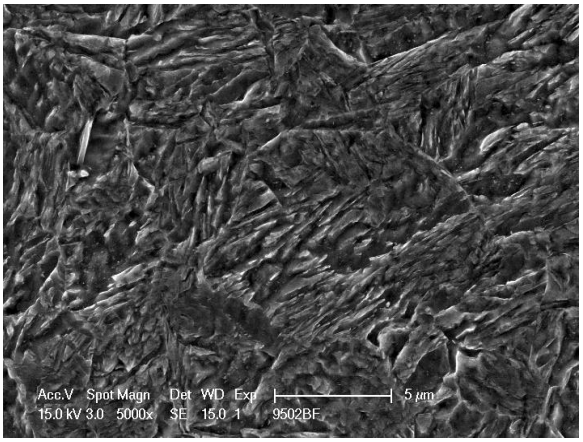

Figure 55. Another SEM results of sample 950_2BF, showing martensite microstructure exist dispersedly in several regions

Figure 54 and Figure 55 show bainite microstructure and martensite microstructure, respectively, for sample 950_2BF. The results agree with prior results from other samples in theoretical manner.

4.3 ELECTRON BACKSCATTER DIFFRACTION

OM and SEM allowed for morphological study in the microstructure. However, the internal structure and also evident of formation for flash bainite still needed to be further confirmed. Electron Backscatter Diffraction (EBSD) is another technique that has been utilized in this research and hence, giving more details on grain orientation and grain boundary angle. Four samples (950 °C heat-treated samples) with flash bainite have been observed using this technique. The results can be seen in Figures 56-60.

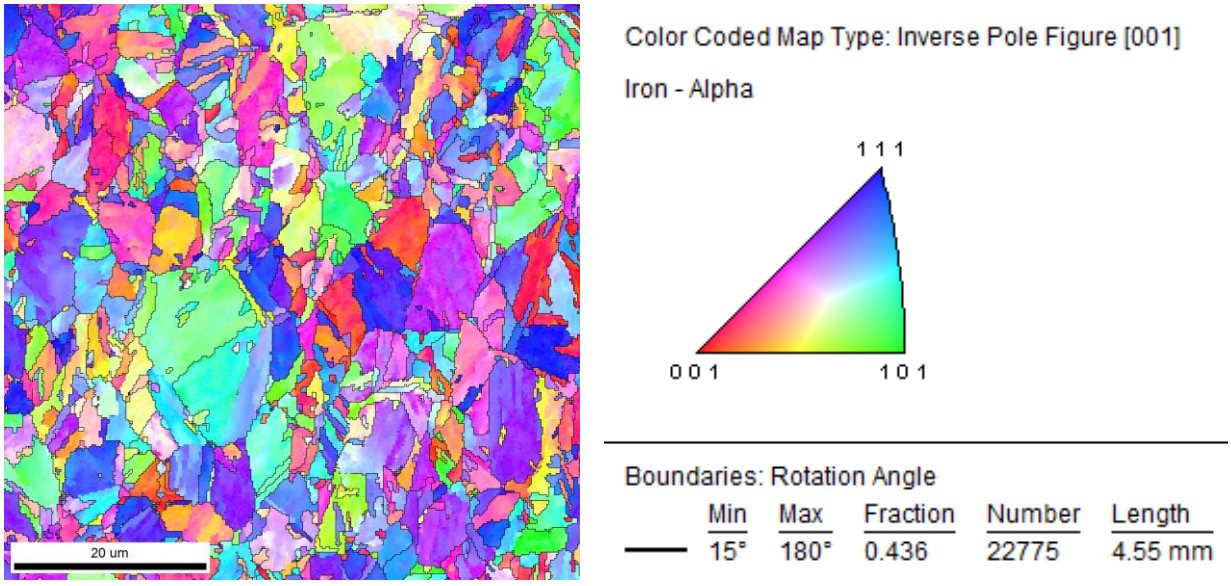

Figure 56. Inverse Pole Figure showing high angle grain boundary for sample 950_2AS with its key

Figure 56 shows high angle grain boundary for sample 950_2AS. The black solid line represents line of high angle boundary. As a result, some of high angle boundary occurs inside austenite grains. The strips of high angle grain boundary inside austenite grains represent the characteristics of bainitic ferrite microstructure [41]. This result conforms to the results obtained from SEM technique. Moreover, the total length of high angle grain boundary is 4.55 mm.

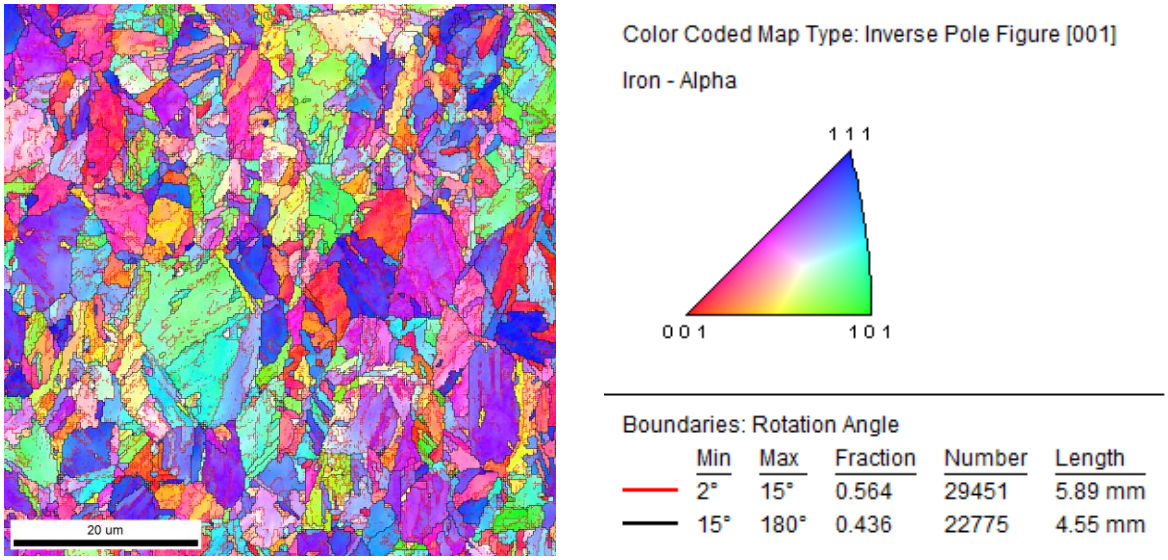

Figure 57. Inverse Pole Figure showing both high and low angle grain boundary for sample 950_2AS with its key

Figure 57 provides information about grain boundary length for both high and low angle grain boundary (small red lines). The total length for low angle grain is 5.89 mm. One dislocation in one grain reflected on EBSD mapping is small angle grain boundary. Small angle grain boundary density is approximated to dislocation density. High dislocation density means high strength and hardness of materials. This means that, higher ratio of small angle grain boundary will result in higher strength and hardness in steels [42].

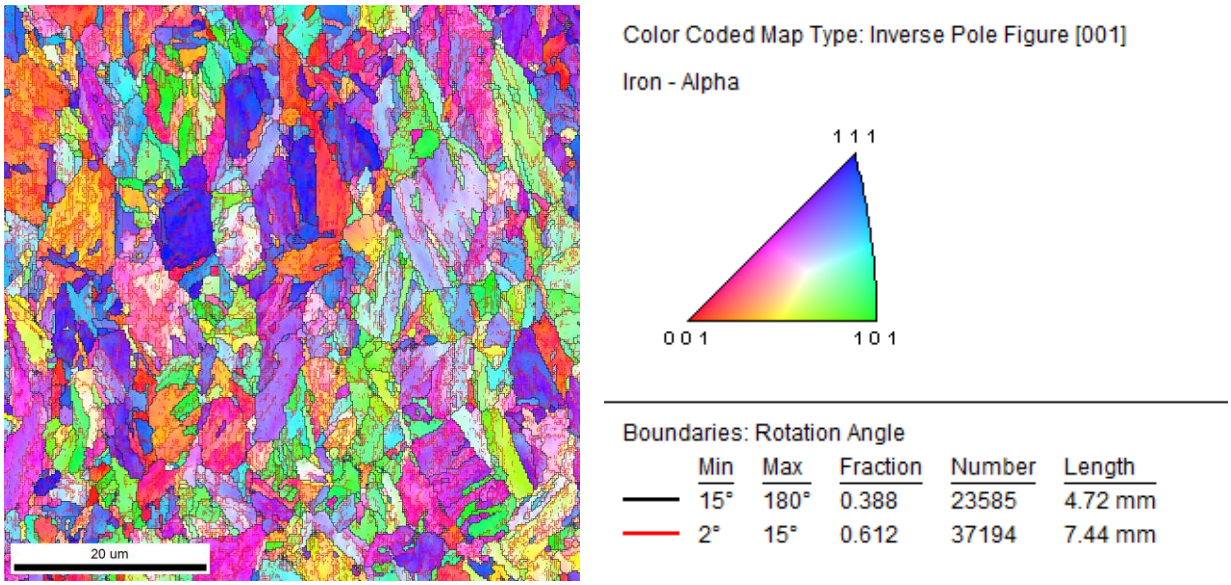

Figure 58. Inverse Pole Figure showing both high and low angle grain boundary for sample 950_2AF with its key

Figure 58 shows another result for sample 950_2AF, both high and low angle grain boundaries. The sample result in higher ratio of small angle grain boundary, compared to sample 950_2AS. This means that the strength and hardness value should also be higher.

Another parameter that can be obtained from EBSD experiment is Kernel Average Misorientation. KAM is calculated within a kernel instead of a grain, so the misorientations between all neighboring points within kernels are averaged. The grain boundary effect is neglected in this case to avoid outstandingly high values. Figure 59 and 60 show KAM profile of samples 950_2BS and 950_2BF. KAM index can further identify the small angle grain boundary density and hence, identifying dislocations density. Table 5 summarizes the value of small angle grain boundary length; high angle grain boundary length; the ratio and KAM average values [39].

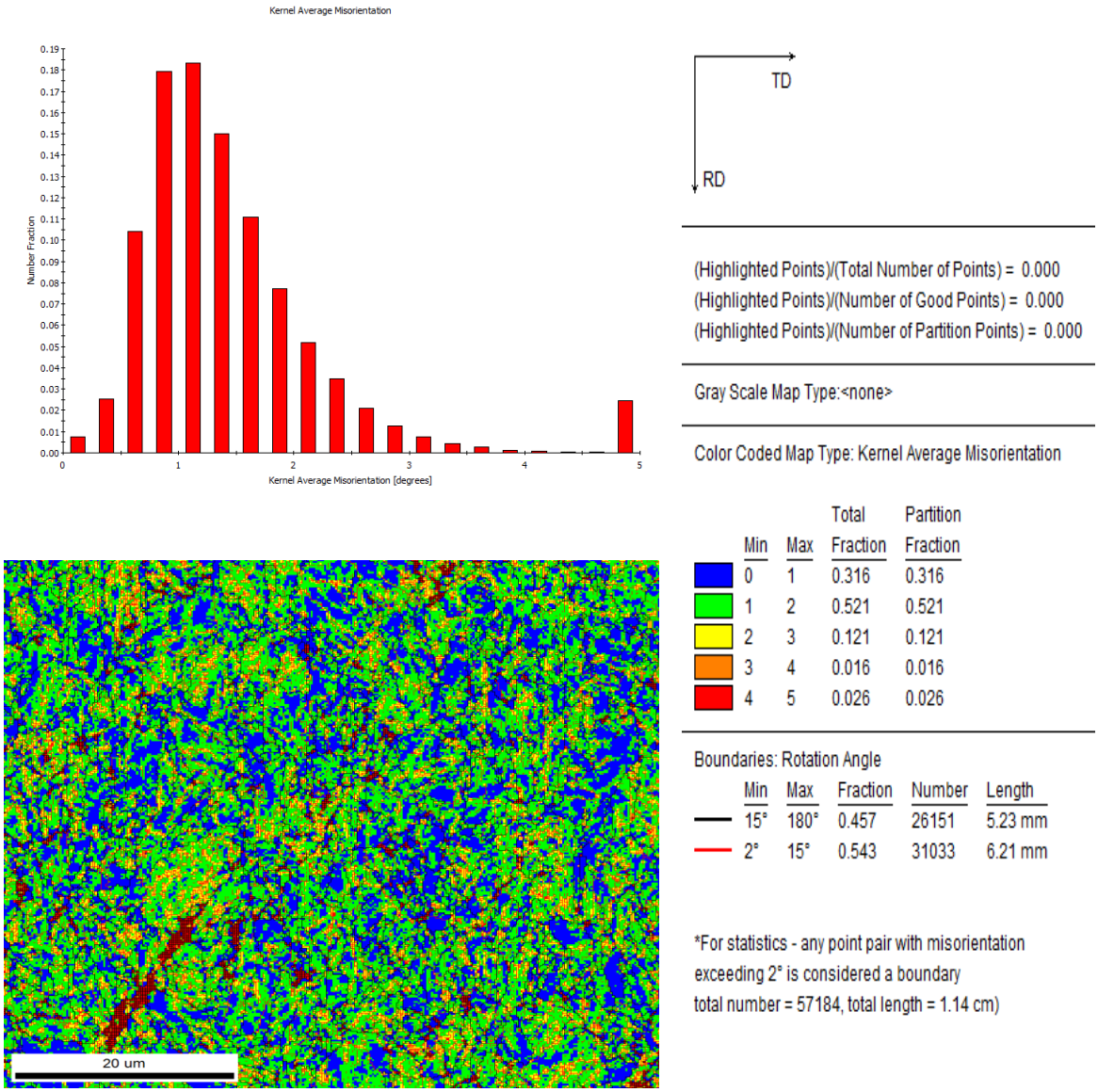

Figure 59. Kernel Average Misorientation (KAM) result for sample 950_2BS

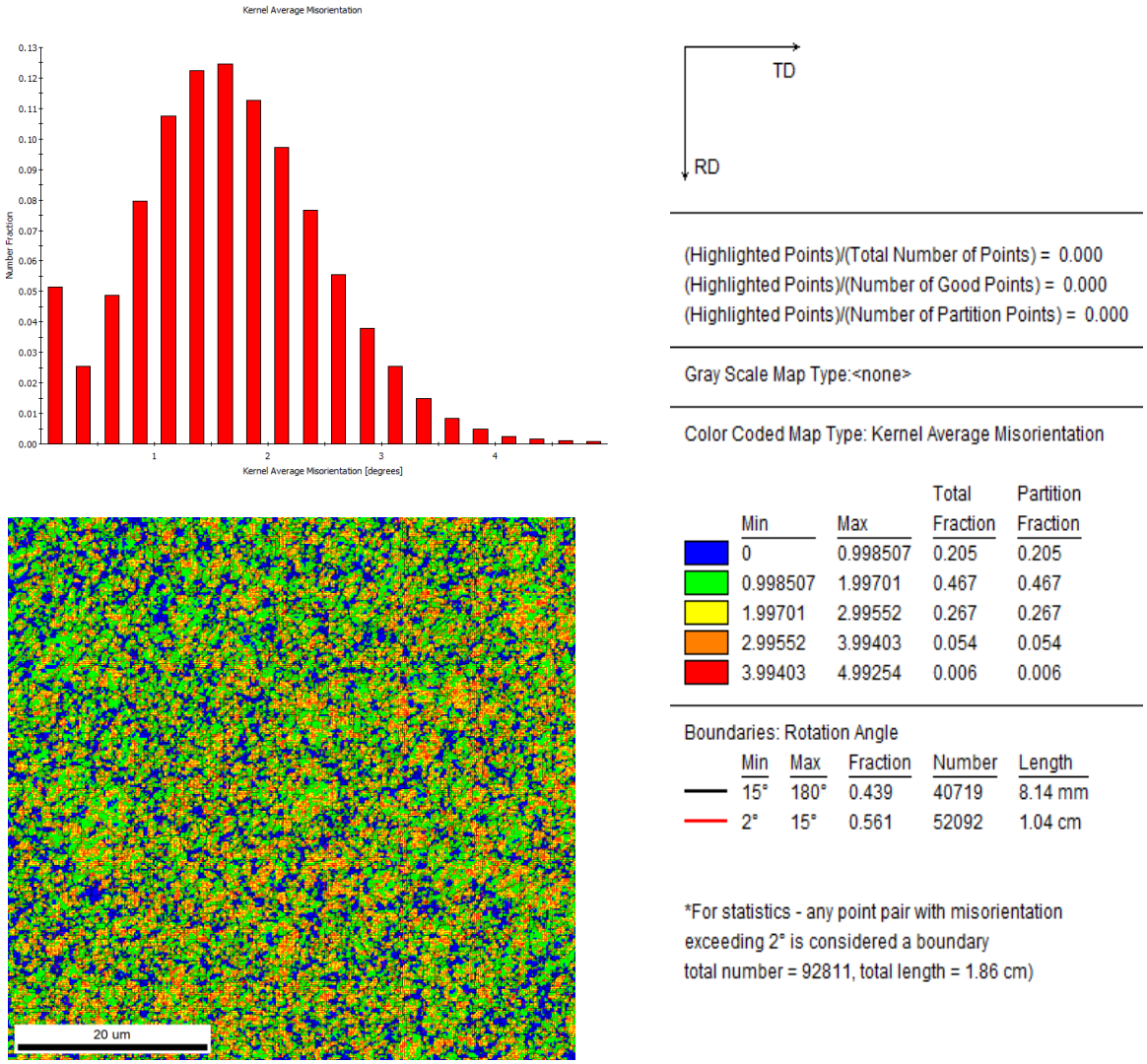

Figure 60. Kernel Average Misorientation (KAM) result for sample 950_2BF

Table 5. Summary of Grain Angle Boundary result

Sample	High Angle Grain Boundary Length (mm)	Low Angle Grain Boundary Length (mm)	Ratio (Low/Total)	KAM
950_2AS	4.55	5.89	0.56	1.38
950_2AF	4.72	7.44	0.61	1.52
950_2BS	5.23	6.21	0.54	1.44
950_2BF	8.14	104	0.93	1.66

4.4 VICKERS HARDNESS TEST

The hardness test has been done to all samples to ensure the mechanical properties of the final microstructure. The hardness results can be summarized within the table below. (Table 6)

Table 6. Vickers Hardness Test with 300 gf results of 12 samples

Steels	Heat Treatment	Hardness (HV)
2A	950 °C, Slow Rate	383.06
	950 °C, fast rate	398.5
	1050 °C, slow rate	383.49
	1050 °C, fast rate	376.08
	1150 °C, slow rate	367.38
	1150 °C, fast rate	387.70
2B	950 °C, Slow Rate	387.07
	950 °C, fast rate	385.39
	1050 °C, slow rate	386.39
	1050 °C, fast rate	363.58
	1150 °C, slow rate	363.08
	1150 °C, fast rate	396.83

The results of hardness test show outstandingly high hardness value, especially for 4 flash bainite samples. Compare to hardness value for typical for cold-rolled AISI 1010 steel (0.1 wt% C), 270 HV, an average value of 385 HV is exceptionally high. This is due to the fact that there are a lot of martensites in the microstructure. However, it should be noted here that flash bainite (950 °C heat-treated samples**)** has an even higher hardness value when compared to 100% martensite microstructure (1050 and 1150 °C heat-treated samples). This emphasizes the performance of flash bainite microstructure, and also, the essence of flash process for the steel industry.

4.5 COMPARISONS

4.5.1 Compared to Typical Flash Bainite

The bainite developed in this research has been studied thoroughly in order to differentiate the characteristics when compared to typical bainite or even typical flash bainite. It should be noted that in [3] and [4], the characteristics of bainite developed from typical flash process have never been extensively discussed. The work of Cola, [3] and [4], mainly focused on mechanical properties and discussed conceptually about bainite microstructure. The fraction of bainite has been measured but never been discussed in morphological side of view. The mechanism of formation of bainite in [4] and this research seems similar. The explanation of the carbon concentration gradients as a source for bainite (low carbon) and martensite (high carbon) formations can be applied for both research. The mechanical properties tested in [4] show outstandingly high value of hardness for the flash bainite (~550-650 HV) for 4130 steels. This is also the case in this research, as the average value of hardness value in flash bainite samples is around 385-393 HV for carbon content of only 0.1 percent. However, the difference is the fraction of bainite developed in the microstructure and may also be the case for the type of bainite.

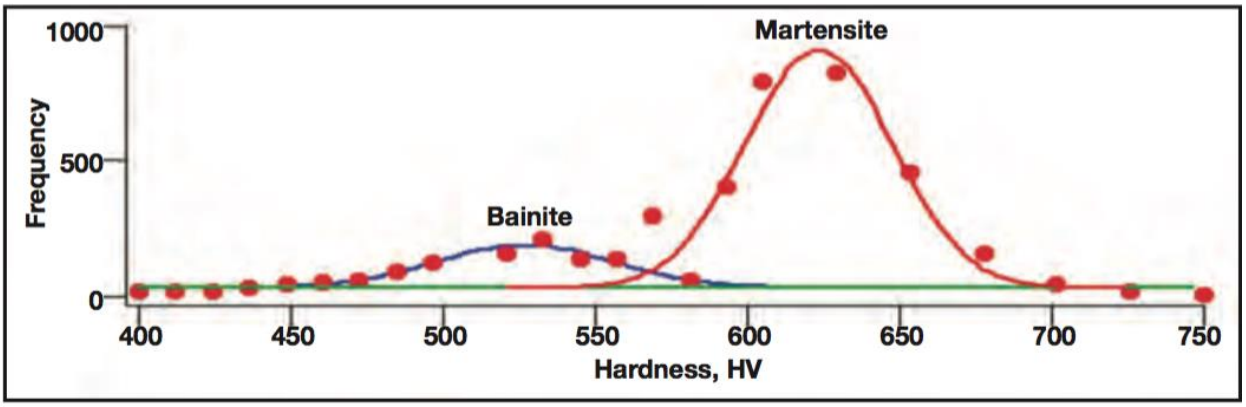

Figure 61. The nano-hardness results of 4130 flash-processed steels [4]

4.5.2 Compared to Typical Bainite

However, in Liang's work, [41], the microstructure and morphological appearances of bainite have been intensively studied. In Liang's work, bainitic ferrite microstructures with various heating rates have been studied and discussed. The effects of cooling rate to the low carbon bainite were thoroughly studied. Faster cooling rates resulted in higher fraction of bainite laths and also more bainitic ferrite was observed. The cooling rate of 40 °C/s showed a clear sign of change for bainite characteristics in the final microstructure as it changed shape to be more lath-like form. This is also the case for this current study. In this research the cooling rates being used were 100 and 200 °C/s, notably higher than in [41]. The results in microstructure obtained from SEM showed clear shape of several lath-like and plate-like microstructures. The morphology of bainite found in this research seems to comply with the conclusions from Liang's

work. Hence, it could be concluded here that the bainite developed here is bainitc ferrite. However, it should be noted here that the difference between carbon contents (0.06 wt% C and 0.1 wt% C) and also martensite fractions in the steels and final microstructures, may led to the difference in mechanical properties of the steels in the end.

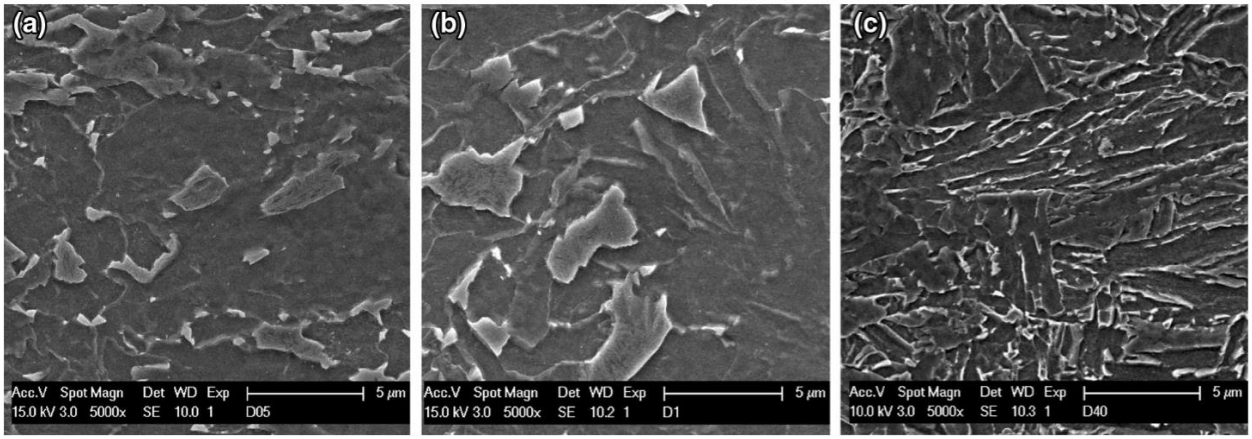

Figure 62. The bainite morphology from different cooling rates from 0.5 °C/s, 1.0 °C/s and 40 °C/s (From left to right, respectively) [41]

5.0 CONCLUSIONS

Flash process and flash bainite is a relatively new heat treatment process and microstructure that need to be further studied to develop more understanding and information about them. Some observations have been made, both by an inventor, Cola, and other researchers. This research aims to provide more understanding in morphological and microstructural aspects. The results show that the bainite microstructures are developed in 4 samples, heat-treated at 950 °C, both fast and slow heat treatment rates. The bainite developed in the samples was due to the incomplete carbide dissolution during heating and holding stages in heat treatment. The incomplete carbides dissolution resulted in carbon concentration gradients and hence, promoting 2 types of microstructure in the end. The shorter the heating time, the higher the bainite ratio in the final microstructure. From SEM results, the type of bainite can be studied. Morphologically and apparently, the bainite developed in this research appeared to resemble bainitic ferrite type. The sheaves of plate-like bainite formed from the grain boundary and extended into austenite grains. Martensite microstructure was found dispersedly in the samples, since the fraction of martensite is higher. EBSD results also show that the dislocation density within the samples with flash bainite is reasonably similar and high. This is also the case for KAM averaged value. Both dislocation density and KAM values are directly related to strength and hardness of materials.

This is why the flash bainite samples showed outstandingly high Vicker hardness results, even when compared to full martensite samples (1050 °C and 1150 °C heat-treated samples).

BIBLIOGRAPHY

[1] Y. Gong, M. Hua, J. Uusitalo and A. DeArdo, "Improving the Strength-Ductility Balance in High-Strength Dual-Phase Steels Through the Addition of Vanadium," Galvatech 2015 Proceedings by AIST, 2015.

[2] World Steel Association, "World Steel in Figures," 2015.

[3] Lolla, B. Alexandrov, S. Babu and G. Cola, "Towards Understanding the Microstructure Development During Flash Heating and Cooling of Steels," Materials Science and Technology, 2008.

[4] J. G.M. Cola, "Flash Bainite Process," Adventures in the Physical Metallurgy of Steels, 2013.

[5] H. Bhadeshia and R.W.K. Honeycombe, Steels: Microstructure and properties 3rd ed., Amsterdam; Boston; London: Butterworth-Heinemann, 2006.

[6] J. Guimaraes and P. Rios, "Microstructural Path Analysis of Martensite Dimensions in FeNiC and FeC Alloys," Mat. Res., vol. 18, no. 3 Sao Carlos, May/June 2015.

[7] R. Honeycombe, Steels: Microstructure & Properties, 1987.

[8] E. Davenport and E. Bain, "Transformation of austenite at constant subcritical temperatures," Trans. Am. Inst. Min. Engng., pp. 90:117-154, 1930.

[9] A. Hultgren, J. Iron Steel Inst., pp. 114:421- 422, 1926.

[10] M. Hillert, "The Growth of ferrite, bainite and martensite. Internal report," Swedish Institute for Metals Research, Sweden, 1960.

[11] A. Borgenstam, M. Hillert and J. Agren, "Metallographic evidence of carbon diffusion in the growth of bainite," Acta Mater., pp. 57: 3242-3252, 2009.

[12] W. Jellinghaus and F. Wever, "Transofrmation kinetics of austenite II.," Mitt. Kaiser-Wilhelm-Inst. Eisenforch, 1932.

[13] P. Chevenard and A. Portevin, "The transformations during the cooling of steels," P. Compt. Rend, p. 204:772, 1937.

[14] C. Zener, "Kinetics of the decomposition of austenite," Trans. Am. Inst. Min. Metall. Engng., pp. 167:550-595, 1946.

[15] J. Vilella, G. Guellich and E. Bain, "On naming the aggregate constituents in steels," Trans. ASM, pp. 24:225-261, 1936.

[16] J. Robertson, "The microstructure of rapidly cooled steel," J. Iron. Steel Inst., pp. 119:391-424, 1929.

[17] R. Mehl, "Mechanism and rate of decomposition from austenite in hardenability of alloy steels," ASM, pp. 1-65, 1939.

[18] A. Hultgren, "Isothermal transformation of austenite," Trans. ASM, pp. 39:915-989, 1947.

[19] M. Hillert, "Paraequilibrium Technical Report," Swedish Institute for Metals Research, Stockholm, Sweden, 1953.

[20] A. Jena and M. Chaturvedi, Phase Transformations in Materials, Prentice-Hall, 1992.

[21] H. Bhadeshia, Bainite in steel: Transformation, microstructure and properties, London, United Kingdom: IOM Communications Ltd, 2001.

[22] Durand-Charre and Madeleine, Microstructure of steels & Cast Irons, Springer, 2004.

[23] A. Barbacki and Z. Lawrynowicz, "Feature of bainite transformation in steels," Advances in Materials Science, vol. 2, no. 1, November 2002.

[24] P. Suikkanen, "Development and processing of low carbon bainitic steels," In Department of Mechanical Engineering, p. 482, 2009.

[25] Troiano and T. Lyman, A.R. Trans., vol. ASM 37, pp. 402-448, 1946.

[26] A. Kamada, N. Koshizuka and T. Funakoshi, T. Trans., vol. ISIJ 16, p. 407, 1976.

[27] P. Pickering and K. Irvine, "F.B. ISI Spec. Rep.93," ISI, London, 1965.

[28] W. Leslie, Physical Metallurgy of Steels, Tokyo, Japan: McGraw-Hill Kogakusha, 1982.

[29] A. ". Khan, The effect of morphology on the strength of copper-based martensites (1 ed.), Leuven, Belgium: University of Leuven, 1972.

[30] H. Bhadeshia, "Austenite grain size and the martensite-start temperature," Scripta Matrerialia 60, pp. 493-495, 2009.

[31] H. Bhadeshia, Geometry of Crystals (with corrections ed.), London: Institute of Materials, 2001.

[32] M. F. Ashby and David R.H. Jones, Engineering Materials 2 (with corrections ed.), Oxford, United Kingdom: Pergamon Press, 1992.

[33] L. Mrosdorf, C. Tasan, D. Ponge and D. Raabe, "3D Structural amd atomic-scale analysis of lath-martensite: Effect of the transformation sequence," Acta Materialia 95, pp. 366-277, 2015.

[34] M. Baumeister and A. Baumeister, Standard Handbook for Mechanical Engineers, 8th ed., McGraw Hill.

[35] J. D. Verhoeven, Steel Metallurgy for the Non-Metallurgist, American Society for Metals, 2007.

[36] S. Morito, X. Huang, T. Furuhara, T. Maki and N. Hansen, Acta Materialia. 54, pp. 5323-5333, 2006.

[37] G. Vigilante, M. Hespos and S. Bartolucci, "Technical Report ARWSB-TR-11011: Evaluation of Flash Bainite in 4130 Steel," Benet Laboratories, New Jersey, USA, 2011.

[38] H. Zakerinia, A. Kermanpur and A. Najafizadeh, "Color metallography; a suitable method for characterization of martensite and bainite in multiphase steels," International Journal of ISSI, vol. 6, no. 1, pp. 14-18, 2009.

[39] S. I. Wright, M. M. Nowell and D. P. Field, "A Review of Strain Analysis Using Electron Backscatter Diffraction," Microscopy and Microanalysis, vol. 17, pp. 316-329, 2011.

[40] C. Bampton, J. Wert and M. Mahoney, "Heating Rate Effects on Recrystallized Grain Size in Two Al-Zn-Mg-Cu Alloys," Metallurgical Transactions A, vol. 13, no. 2, pp. 193-198, February 1982.

[41] A.J.DeArdo and X. Liang, "A Study of the Influence of Thermomechanical Controlled Processing on the Microstructure of Bainite in High Strength Plate Steel," Metallurgical and Materials Transactions A, vol. 45A, October 2014.

[42] F. Humphreys and M. Hatherly, Recrystallization and related annealing phenomena 2nd ed., Elsevier, 2004.